frontiers in GENETICS

HYPOTHESIS AND THEORY ARTICLE
published: 20 September 2011
doi: 10.3389/fgene.2011.00065

The functional consequences of relative substrate specificity in complex biochemical systems

Yan Zeng*

Department of Pharmacology, Masonic Cancer Center, University of Minnesota, Minneapolis, MN, USA

Edited by:
Josselin Noirel, University of Sheffield, UK

Reviewed by:
Necmettin Yildirim, New College of Florida, USA
Anne-Gaëlle Planson, Institute of Systems and Synthetic Biology, France
Paul Dobson, University of Sheffield, UK

****Correspondence:***
Yan Zeng, Department of Pharmacology, University of Minnesota, 6-120 Jackson Hall, 321 Church Street SE, Minneapolis, MN 55455, USA.
e-mail: zengx033@umn.edu

A biochemical activity, that is, enzymatic reaction or molecular interaction, frequently involves a molecule, for example, an enzyme, capable of interacting with numerous substrates or partners. Specificity is a fundamental property of biochemical activities, and relative specificity refers to the situation whereby a molecule interacts with multiple substrates or partners but with different affinities. Here, a hypothesis is proposed that any molecule, such as an enzyme, would have a range of preferences or relative specificity for its many native substrates, which differentially impacts the phenotypes of these substrates and hence shapes the relevant biological processes *in vivo*. While the mechanisms underlying the specific recognition between enzymes and individual substrates have been studied extensively, whether any enzyme exhibits intrinsic selectivity toward its ensemble of substrates is often overlooked, and whether this selectivity has any functional consequences is much less appreciated. There are, however, several lines of evidence in the literature that are consistent with the hypothesis and reviewed here. Furthermore, this hypothesis is supported by our analyses of a number of diverse biochemical systems at a large scale. Thus, the human microRNA processing machinery possesses relative specificity toward its hundreds of substrates, which might contribute to differential microRNA biogenesis; the promoter binding affinity of the transcription factor Ndt80 might regulate Ndt80 target mRNA expression in the budding yeast; Cdk1 kinase specificity might lead to variable substrate phosphorylation *in vivo*; and the density of HuR deposition to its thousands of RNA targets might partly explain differential RNA expression in human cells. It is proposed, therefore, that relative specificity is a universal property of complex biochemical systems and that the hypothesis could denote a general principle in biology.

Keywords: biochemical activity, relative specificity, substrate selectivity, regulatory function

INTRODUCTION

Specificity in biochemical activities has two components, absolute specificity and relative specificity. For absolute specificity, a molecule, symbolized as E here, recognizes a group of substrates or interacting partners (symbolized as {S}) but not any others. For relative specificity, an E interacts with more than one cognate {S} differentially. The functional implication of absolute specificity is self-evident, so the focus here is on relative specificity, although absolute specificity can be viewed as an extreme case of relative specificity. This paper addresses a hypothesis that an E has a range of affinities or preferences for its many {S}, and that such selectivity differentially impacts the {S} to influence the underlying biological processes at a large scale *in vivo* (**Figure 1A**). Below, I will first explain the hypothesis in more detail. While the proposition appears intuitively plausible, it is actually understudied and not grounded in real data in most biochemical systems. Next, potential evidence in the literature will be summarized. Our own work will then be presented to further support the hypothesis and to demonstrate strategies to test the hypothesis directly. Lastly, the implications of the hypothesis will be discussed.

RELATIVE SUBSTRATE PREFERENCES ARE NOT WELL UNDERSTOOD AT THE SYSTEMS LEVEL

The number of {S} varies greatly with E. For example, hemoglobin binds a handful of {S}, e.g., O_2, CO_2, CO, with CO having a higher affinity than O_2 for hemoglobin, leading to a textbook consequence. On the other hand, the ribosome and RNA polymerase II have tens of thousands of {S} in multicellular organisms. In the middle of the spectrum, an enzyme may catalyze the conversion of dozens or hundreds of substrates, and a molecule may interact with a large number of partners; some examples are protein kinases, transcription factors, and microRNAs (miRNAs). The hypothesis of interest is broadly applicable but was conceived with complex systems in mind wherein an E has at least dozens or hundreds of cognate {S}. The significance of specific recognition sequences in individual or model targets has been extensively investigated for E such as kinases and transcription factors, but whether an E possesses selectivity toward its ensemble of {S} is often unknown, and whether this selectivity has any *in vivo* relevance is seldom reported in the literature. For example, protein kinases and transcription factors typically recognize degenerate sequences in hundreds of native {S}, so it is plausible yet hardly reported that, based on

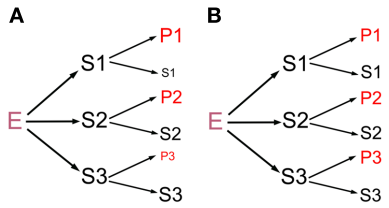

FIGURE 1 | Schematics of how an E interacts with {S}, represented by S1, S2, and S3. The interactions yield the respective products P1, P2, and P3, with the remaining S1, S2, and S3. The letter size symbolizes the abundance of S and P, with the starting S1–S3 being equal for simplicity. **(A)** E discriminates amongst S to yield different amounts of P1, P2, and P3, as the central hypothesis predicts. **(B)** E interacts with S1–S3 identically, a commonly assumed situation. Because S and P likely have different activities *in vivo*, **(A)** and **(B)** will lead to different functional outcomes downstream.

their sequences, some {S} would be better phosphorylated or transcribed than others *in vivo*. Additionally, do the core transcription machinery and the core translation machinery possess any innate preferences toward their tens of thousands of targets genes and mRNAs, respectively, and do the preferences contribute to differential gene expression *in vivo*? Components of these machineries might have isoforms and be differentially expressed, which is regulatory in nature (Goodrich and Tjian, 2010; Kondrashov et al., 2011). The hypothesis formulated here, however, differs from other theories by projecting that regulation can originate at the most basic level from the biased interactions between a single E and its vast number of {S}.

There is a dearth of studies that explicitly address the above or analogous questions, for two reasons. The first is that the potential, regulatory role of E:{S} selectivity is often overlooked. By default, an E is frequently portrayed to operate passively or constitutively, doing an assembly line-like task on its entire set of {S}, regulated only from outside of the system (**Figure 1B**). The second reason is that it is difficult to study the phenomena in complex systems. Firstly, we usually do not know all or most of the genuine {S} for any E. Secondly, {S} or the products *in vivo* must be quantified at a large scale, but the essential genomics or proteomics tools were not available until the late 1990s. Thirdly, a representative assay might not exist to characterize biochemical interactions *in vitro*. For example, only a few artificial or authentic {S} have been tested using the *in vitro* transcription or translation systems, and the products usually do not phenocopy full-length pre-mRNAs or proteins typical *in vivo*. As a result, there are few reports of E discriminating amongst its large set of {S}. Lastly, one has to isolate the effect of E on {S}, as {S} are invariably controlled by multiple factors besides E *in vivo*. Thus, even if an E's relative specificity toward a small number of {S} *in vitro* correlates with the phenotypes of {S} *in vivo*, it remains possible that the correlation results from the fortuitous action of factors other than the E.

POTENTIAL SUPPORTING EVIDENCE IN THE LITERATURE

Despite the challenges, there is evidence in the literature that might support the hypothesis in complex biochemical systems. An example is eIF4E, which binds the 5′ m^7GpppN cap of mRNAs to initiate mRNA scanning and translation (Sonenberg, 2008). All capped mRNAs are eIF4E substrates, but eIF4E overexpression preferentially stimulates the translation of a subset of mRNAs that promote tumorigenesis in mammalian systems. These mRNAs often have a long and stable 5′ untranslated region that presumably requires elevated eIF4E activity, although the direct mRNA selectivity of eIF4E has not been extensively examined *in vitro*. A transcript-specific role has also been ascribed to ribosomal proteins (Kondrashov et al., 2011; Topisirovic and Sonenberg, 2011). Deficiency in ribosomal protein L28 reduces the translation of a subset of Hox mRNAs in mouse embryos, which is not observed in mutants of several other ribosomal proteins (Kondrashov et al., 2011). Likewise, mutations of general transcription factors differentially impact the expression of distinct sets of genes (Holstege et al., 1998). The origin of the selectivity of L28 or general transcription factors, however, is unknown.

Another example is ligand–receptor interaction. Distinct agonists ({S}) can differentially impact downstream signaling pathways even when bound to the same receptor (E), e.g., the μ-opioid receptor, β2-adrenergic receptor, vasopressin, serotonin, and dopamine receptors (reviewed in Urban et al., 2007). The concepts of intrinsic efficacy, functional selectivity, or agonist-selectivity signaling have been proposed to explain this phenomenon (Urban et al., 2007). How E discriminates amongst {S} is not well characterized, but it likely necessitates E to adopt multiple active conformations upon binding by different {S}. Even less understood is how these conformations could differentially activate downstream signaling molecules, quantitatively or qualitatively. An analogous mechanism may partially explain the multifunctionality or promiscuity of other proteins, e.g., the cytochrome P450 enzymes (Khersonsky and Tawfik, 2010; Atkins and Qian, 2011). The general explanation is that a protein (E) exists in a multiplicity of conformations due to inherent structural plasticity. {S} may bind it with different affinities at overlapping but non-identical sites to form complexes with different conformations, and the {S} reactive groups may position in the complexes differently, thereby affecting the subsequent catalysis or product release. Nevertheless, in most cases we probably do not even realize the full spectrum of substrates for such E, and a single molecule can be the substrates of several enzymes in a cell or tissue specific manner, which hampers the global analysis of relative specificity *in vitro* and *in vivo*.

The most revealing case is perhaps the HuR protein, which stabilizes RNAs by binding preferentially to short uridine stretches. Lebedeva et al. (2011) and Mukherjee et al. (2011) identified HuR substrates at the global scale and showed that HuR has thousands of RNA targets with variable, potential HuR binding sites and HuR association in cells, and that the degree of HuR binding correlates with HuR-dependent stability of the target RNAs.

While these studies reported that E:{S} interactions can lead to distinct effects depending on {S}, the phenomena have not been generalized, and the detailed mechanism is unavailable with the exception of HuR (but see below). This is largely due to the lack of suitable *in vitro* biochemical assays or detailed, structural data, leaving open alternative explanations.

REGULATION OF miRNA EXPRESSION BY THE GENERAL miRNA PROCESSING MACHINERY

The rationale behind our hypothesis is that relative specificity is likely a universal, direct, and natural consequence when an E has to interact with many native {S} with different sequences or structures in any complex system, and that *in vivo* phenotypes can partly be explained by the relative specificity of the underlying biochemical activities. Our own work has aimed to directly test this hypothesis. First we studied the biogenesis of miRNAs. miRNAs are a class of ∼22-nucleotide-long RNAs, in mammals encoded by hundreds of known miRNA genes (Ambros, 2004; Newman and Hammond, 2010). A canonical miRNA is initially transcribed as part of a long primary transcript. An RNase called Drosha cleaves this transcript to liberate a hairpin precursor of ∼60 nucleotides. Dicer, another RNase, cleaves the precursor to produce an ∼22 basepair RNA duplex intermediate. Subsequently, an Argonaute (Ago) protein binds to the duplex and selects the mature, single-stranded miRNA. The Ago:miRNA complex then functions by repressing target gene expression downstream.

We investigated the cleavage of hundreds of human primary miRNA substrates by Drosha *in vitro* (Feng et al., 2011). Drosha (E) cleaves these RNAs ({S}) with different efficiencies, which positively correlates with the relative expression levels of the corresponding mature miRNAs *in vivo*, and the specificity could be partially explained by different structural properties of the substrates. Considering the well-known biochemical function of Drosha, we suggested that Drosha selectivity determines, to a significant extent, whether a transcript encodes a miRNA or not, and how efficiently a miRNA is produced *in vivo* (Feng et al., 2011).

In a related study, we showed that stable Ago2 overexpression increases or decreases the maturation of distinct miRNAs in human cells (Zhang et al., 2009). This result is analogous to that of eIF4E. Because Ago2:miRNA complexes inhibit the expression of target mRNAs, the differential effects of Ago2 might be accounted for by the interdependence of the expression of specific mRNAs and miRNAs (Zhang et al., 2009).

SELECTIVITY IN Ndt80 AND Cdk1 FUNCTIONS

Our Drosha study combined *in vitro* assays and *in vivo* data analysis to explicitly test the hypothesis. No other biological systems, however, have been examined in a similar and deliberate manner. The best functional genomics studies have been performed in *S. cerevisiae*, so I carried out literature search, data mining, and analysis for this model organism.

Ndt80 is a transcription factor involved in middle gene induction (∼5 h) during sporulation (Chu and Herskowitz, 1998). Jolly et al. (2005) showed that Ndt80 binds DNA with nucleotide preferences in an *in vitro* binding assay, generated a corresponding, position weight matrix (PWM), and then curated a list of 145 known and predicted Ndt80 target genes. For this analysis, the potential Ndt80 binding sites in these 145 genes were retrieved using the YEASTRACT database (Teixeira et al., 2006), and their PWM scores calculated (**Table A1** in Appendix). If a gene has more than one potential Ndt80 site, the highest PWM score was used as the representative. Not surprisingly, the target genes have variable PMW scores (**Table A1** in Appendix), so Ndt80 could associate with the promoters with different affinities or probabilities, suggestive of relative specificity *in vivo*. Next, mRNA expression data were extracted from Chu et al. (1998) where yeast gene expression from 0 to 11.5 h after the initiation of sporulation was determined by microarray analyses (**Table A1** in Appendix). The PWM scores were then correlated with target mRNA expression at the different time points (SPSS, IBM). At 0 h, the Spearman rank correlation coefficient $\rho = 0.008$, p value $= 0.93$; at 0.5 h, $\rho = -0.013$, $p = 0.88$; at 2 h, $\rho = 0.077$, $p = 0.36$; at 5 h, $\rho = 0.35$, $p = 0.00002$; at 7 h, $\rho = 0.30$, $p = 0.0003$; at 9 h $\rho = 0.31$, $p = 0.0002$; at 11.5 h, $\rho = 0.29$, $p = 0.0004$. The positive correlation peaks at 5 h, consistent with the known function of Ndt80 (Chu and Herskowitz, 1998). This result suggested that Ndt80 binding specificity, determined *in vitro*, could translate to differential target gene expression *in vivo*.

The other example is protein phosphorylation by *S. cerevisiae* Cdc28, or Cdk1, which controls cell cycle progression. Ubersax et al. (2003) showed that the mitotic Cdk1 phosphorylates hundreds of proteins *in vitro*. The extent of substrate phosphorylation, or *P*-scores, ranged over seven orders of magnitude, which cannot be explained by the differences in possible phosphorylation sites. Cdk1, therefore, discriminates amongst {S} *in vitro*, just like Drosha.

Does this specificity impact the phosphorylation levels of Cdk1 substrates *in vivo*? Using mass spectrometry, Holt et al. (2009) identified phosphorylation sites in hundreds of Cdk1 substrates in especially cells arrested by the overexpression of a stable mitotic cyclin. For this analysis the Signal/Noise (S/N) ratio was used as a proxy for phosphorylation *in vivo*, although data from Holt et al. (2009) did not allow for normalization against total protein expression. For a protein with more than one phosphopeptide, the sum of all the S/N ratios was used to represent its phosphorylation (**Table A2** in Appendix). *P*-scores correlated positively and significantly with S/N ratios: $n = 144$, $\rho = 0.29$, $p = 0.0005$, so Cdk1 specificity *in vitro* (Ubersax et al., 2003) might partially explain differential substrate phosphorylation *in vivo* (Holt et al., 2009).

The analyses of Ndt80 and Cdk1 functions demonstrated for the first time a global correlation between the *in vitro* specificity and *in vivo* functions of a transcription factor and a protein kinase, respectively. Does the relative specificity have a physiological impact? Differential miRNA and mRNA expression is presumably regulatory and functionally relevant *in vivo*. And because a phosphoprotein and its non-phosphorylated counterpart often differ in their activity, subcellular localization, and/or stability, Cdk1 might phosphorylate its many substrates to various degrees to regulate cell cycle progression. This is a novel angle to look at Cdk1 functions that merits further investigations.

HuR BINDING AND TARGET RNA EXPRESSION

Lebedeva et al. (2011) and Mukherjee et al. (2011) convincingly demonstrated that the degree of HuR association predicts HuR-dependent RNA stabilization. The authors measured HuR association by RNA sequencing or arrays following HuR immunoprecipitation from cell cultures, and HuR-dependent RNA stabilization by the HuR knockdown strategy. A prediction from our hypothesis, not explicitly tested in these studies, is that HuR specificity positively contributes to the absolute expression levels of target RNAs.

HuR consensus RNA binding sequences are very degenerate and not precisely defined (Levine et al., 1993; de Silanes et al., 2004; Meisner et al., 2004; Ray et al., 2009), so a PWM score might not adequately depict a potential HuR:target interaction. Furthermore, both Lebedeva et al. (2011) and Mukherjee et al. (2011) showed that RNAs ({S}) can vary substantially in their numbers of HuR binding sites, a sign of HuR relative specificity. Consequently, the number of HuR binding sites or its variations were used here to represent HuR:RNA association, and the data of Lebedeva et al. (2011) and Mukherjee et al. (2011) re-analyzed. The strongest correlation was detected between the fragments/read pairs per kilobase of exon per million read pairs, reflecting relative mRNA expression, and the fraction of length covered by binding clusters, reflecting HuR association normalized against transcript size (Table S2 in Lebedeva et al., 2011). For the 4,845 consensus HuR targets, the Spearman rank correlation coefficient is 0.39, $p = 2.6 \times 10^{-171}$; for the 1,216 conservative targets, the coefficient is 0.36, $p = 2.8 \times 10^{-38}$ (Table S2 in Lebedeva et al., 2011). Using the predicted or verified HuR binding site numbers without transcript size normalization yielded positive but less significant correlations to the RNA sequencing or array data (Lebedeva et al., 2011; Mukherjee et al., 2011; data not shown). This new result suggested that the density of HuR deposition best explains the differential expression of HuR target RNAs.

INTERPRETATIONS OF OUR RESULTS

Our studies serve as examples to illustrate how one can test the hypothesis directly. As the first step, one needs to realize that relative specificity is a general and functioning characteristic in any complex systems. In step 2, a biochemical assay, usually with purified components *in vitro*, will examine the interactions between an E and {S} at a large scale. In step 3, a global approach will characterize {S} or the products in cells or *in vivo*. As the last step, a significant statistics correlation is expected between the results from steps 2 and 3. In our work, because the biochemical activities of Drosha, Ndt80, Cdk1, and HuR are firmly established, the observed correlations present strong evidence that the relative biochemical specificity is causal and functional *in vivo*.

Somewhat remarkably, our conclusions were reached despite the complexities in the underlying biological problems and data acquisition. For example, Drosha cleavage efficiencies can only be approximated (Feng et al., 2011), S/N ratio depends on phosphorylation efficiency, peptide extraction or ionization, and protein expression, and PWM gives mere estimates. Concentrations of {S} *in vivo* might deviate greatly from K_m, and {S} will compete for the access to E, which might skew or complicate the effects of E selectivity. Multiple steps and factors influence miRNA maturation, mRNA expression, or protein phosphorylation. Our analyses assumed that the specificity of E was sufficiently independent of all the other contributing factors, such that examining a large number of {S} would enable us to assess statistical significance in the complex processes. No strategy, however, can completely filter out the effects by every interfering factor *in vivo*.

With these considerations, it is not surprising that relatively small correlation coefficients were obtained. There are two angles to look at the numbers. One is that they reflect spurious correlations. Nevertheless, the coefficients are similar to many reported in the literature (e.g., Lackner et al., 2007; Tuller et al., 2010), the correlations are significant in diverse systems, and they can all be explained biochemically. Alternatively, they suggest that the relative E:{S} specificity is only one of myriad factors that contribute to the final phenotype *in vivo*, but it still plays an integral and important role. For example, protein degradation does not contribute to global protein expression as significantly as other factors, but it is arguably still an important regulatory mechanism (Schwanhäusser et al., 2011). Furthermore, for the reasons given above, these coefficients likely underestimate the relationships *in vivo*, and more inclusive and precise measurements and better analytic tools in the future may improve the values and elucidate the true significance of E:{S} specificity.

IMPLICATIONS AND CONCLUDING REMARKS

How biological processes are regulated is a subject of intense investigations yet remains incompletely understood, especially at the systems level. This hypothesis posits that relative specificity is the rule rather than the exception at a global scale such that we must pay more attention to the functional role of substrate preferences in individual biochemical activities. Take a familiar example, to comprehend how genes A, B, C, etc are differentially transcribed, a standard work plan is to identify the relevant chromatin modifiers, specific transcription factors, and RNA-processing complexes. The knowledge is incomplete, however, until we understand their relative affinities or efficacies for the specific genes, elucidate the non-identical impact from RNA polymerase II and the general transcription factors, and quantify their individual contributions.

That biochemical activities regulate biological processes is a truism, and as stated by Mukherjee et al. (2011), "All targets were not quantitatively equivalent." This hypothesis, however, explicates how a certain level of regulation is achieved and brings attention to the regulatory properties of many entities that have been traditionally ignored or greatly underappreciated. Testing the hypothesis for the functions of Drosha, Ndt80, Cdk1, and HuR sheds light on how diverse systems are regulated *in vivo*. In addition, studying global relative specificity has provided new insights into its biological significance. For example, eIF4E selectivity manifests itself in promoting tumorigenesis, agonist-selective signaling may explain, in part, how, e.g., different opioid drugs elicit different physiological responses, and Drosha processing may control the specificity and efficiency of miRNA biogenesis.

To conclude, this paper emphasizes the pervasive, functional role of relative specificity in biochemical activities and outlines a general strategy to analyze its significance in complex systems. Future studies to test the hypothesis will advance our knowledge of how biological processes are regulated and how relative specificity has evolved.

ACKNOWLEDGMENTS

I thank Drs Xiaoxiao Zhang and Yong Feng for work in the laboratory and Drs Paul Graves and Clifford Steer for comments on the manuscript.

REFERENCES

Ambros, V. (2004). The functions of animal microRNAs. *Nature* 431, 350–355.

Atkins, W. M., and Qian, H. (2011). Stochastic ensembles, conformationally adaptive teamwork, and enzymatic detoxification. *Biochemistry* 50, 3866–3872.

Chu, S., DeRisi, J., Eisen, M., Mulholland, J., Botstein, D., Brown, P. O., and Herskowitz, I. (1998). The transcriptional program of sporulation in budding yeast. *Science* 282, 699–705.

Chu, S., and Herskowitz, I. (1998). Gametogenesis in yeast is regulated by a transcriptional cascade dependent on Ndt80. *Mol. Cell* 1, 685–696.

de Silanes, I. L., Zhan, M., Lal, A., Yang, X., and Gorospe, M. (2004). Identification of a target RNA motif for RNA-binding protein HuR. *Proc. Natl. Acad. Sci. U.S.A.* 101, 2987–2992.

Feng, Y., Zhang, X., Song, Q., Li, T., and Zeng, Y. (2011). Drosha processing controls the specificity and efficiency of global microRNA expression. *Biochim. Biophys. Acta* doi: 10.1016/j.bbagrm.2011.05.015. [Epub ahead of print].

Goodrich, J. A., and Tjian, R. (2010). Unexpected roles for core promoter recognition factors in cell-type-specific transcription and gene regulation. *Nat. Rev. Genet.* 11, 549–558.

Holstege, F. C., Jennings, E. G., Wyrick, J. J., Lee, T. I., Hengartner, C. J., Green, M. R., Golub, T. R., Lander, E. S., and Young, R. A. (1998). Dissecting the regulatory circuitry of a eukaryotic genome. *Cell* 95, 717–728.

Holt, L. J., Tuch, B. B., Villén, J., Johnson, A. D., Gygi, S. P., and Morgan, D. O. (2009). Global analysis of Cdk1 substrate phosphorylation sites provides insights into evolution. *Science* 325, 1682–1686.

Jolly, E. R., Chin, C. S., Herskowitz, I., and Li, H. (2005). Genome-wide identification of the regulatory targets of a transcription factor using biochemical characterization and computational genomic analysis. *BMC Bioinformatics* 6, 275. doi: 10.1186/1471-2105-6-275

Khersonsky, O., and Tawfik, D. S. (2010). Enzyme promiscuity: a mechanistic and evolutionary perspective. *Annu. Rev. Biochem.* 79, 471–505.

Kondrashov, N., Pusic, A., Stumpf, C., Shimizu, K., Hsieh, A. C., Xue, S., Ishijima, J., Shiroishi, T., and Barna, M. (2011). Ribosome-mediated specificity in Hox mRNA translation and vertebrate tissue patterning. *Cell* 145, 383–397.

Lackner, D. H., Beilharz, T. H., Marguerat, S., Mata, J., Watt, S., Schubert, F., Preiss, T., and Bähler, J. (2007). A network of multiple regulatory layers shapes gene expression in fission yeast. *Mol. Cell* 26, 145–155.

Lebedeva, S., Jens, M., Theil, K., Schwanhäusser, B., Selbach, M., Landthaler, M., and Rajewsky, N. (2011). Transcriptome-wide analysis of regulatory interactions of the RNA-binding protein HuR. *Mol. Cell* 43, 340–352.

Levine, T. D., Gao, F., King, P. H., Andrews, L. G., and Keene, J. D. (1993). Hel-N1: an autoimmune RNA-binding protein with specificity for 30 uridylate rich untranslated regions of growth factor mRNAs. *Mol. Cell Biol.* 13, 3494–3504.

Meisner, N. C., Hackermüller, J., Uhl, V., Aszódi, A., Jaritz, M., and Auer, M. (2004). mRNA openers and closers: modulating AU-rich element-controlled mRNA stability by a molecular switch in mRNA secondary structure. *Chembiochem* 5, 1432–1447.

Mukherjee, N., Corcoran, D. L., Nusbaum, J. D., Reid, D. W., Georgiev, S., Hafner, M., Ascano, M., Tuschl, T., Ohler, U., and Keene, J. D. (2011). Integrative regulatory mapping indicates that the RNA-binding protein HuR couples pre-mRNA processing and mRNA stability. *Mol. Cell* 43, 327–339.

Newman, M. A., and Hammond, S. M. (2010). Emerging paradigms of regulated microRNA processing. *Genes Dev.* 24, 1086–1092.

Ray, D., Kazan, H., Chan, E. T., Peña Castillo, L., Chaudhry, S., Talukder, S., Blencowe, B. J., Morris, Q., and Hughes, T. R. (2009). Rapid and systematic analysis of the RNA recognition specificities of RNA-binding proteins. *Nat. Biotechnol.* 27, 667–670.

Schwanhäusser, B., Busse, D., Li, N., Dittmar, G., Schuchhardt, J., Wolf, J., Chen, W., and Selbach, M. (2011). Global quantification of mammalian gene expression control. *Nature* 473, 337–342.

Sonenberg, N. (2008). eIF4E, the mRNA cap-binding protein, from basic discovery to translational research. *Biochem. Cell Biol.* 86, 178–183.

Teixeira, M. C., Monteiro, P., Jain, P., Tenreiro, S., Fernandes, A. R., Mira, N. P., Alenquer, M., Freitas, A. T., Oliveira, A. L., and Sá-Correia, I. (2006). The YEASTRACT database, a tool for the analysis of transcription regulatory associations in *Saccharomyces cerevisiae*. *Nucleic Acids Res.* 34, D446–D451.

Topisirovic, I., and Sonenberg, N. (2011). Translational control by the eukaryotic ribosome. *Cell* 145, 333–334.

Tuller, T., Waldman, Y. Y., Kupiec, M., and Ruppin, E. (2010). Translation efficiency is determined by both codon bias and folding energy. *Proc. Natl. Acad. Sci. U.S.A.* 107, 3645–3650.

Ubersax, J. A., Woodbury, E. L., Quang, P. N., Paraz, M., Blethrow, J. D., Shah, K., Shokat, K. M., and Morgan, D. O. (2003). Targets of the cyclin-dependent kinase Cdk1. *Nature* 425, 859–864.

Urban, J. D., Clarke, W. P., von Zastrow, M., Nichols, D. E., Kobilka, B., Weinstein, H, Javitch, J. A., Roth, B. L., Christopoulos, A., Sexton, P. M., Miller, K. J., Spedding, M., and Mailman, R. B. (2007). Functional selectivity and classical concepts of quantitative pharmacology. *J. Pharmacol. Exp. Ther.* 320, 1–13.

Zhang, X., Graves, P. R., and Zeng, Y. (2009). Stable Argonaute2 overexpression differentially regulates microRNA production. *Biochim. Biophys. Acta* 1789, 153–159.

Conflict of Interest Statement: The author declares that the research was conducted in the absence of any commercial or financial relationships that could be construed as a potential conflict of interest.

Received: 24 July 2011; accepted: 30 August 2011; published online: 20 September 2011.

Citation: Zeng Y (2011) The functional consequences of relative substrate specificity in complex biochemical systems. Front. Gene. ***2****:65. doi: 10.3389/fgene.2011.00065*

This article was submitted to Frontiers in Frontiers in Systems Biology, a specialty of Frontiers in Genetics.

APPENDIX

Table A1 | Transcription regulation by Ndt80.

ORF	Position	PWM score	*t*0	*t*0.5	*t*2	*t*5	*t*7	*t*9	*t*11.5
YDR438W	−180	1.13	0.713	1.875	0.883	3.251	8.539	4.887	4.212
YFL011W	−820	0.23359752	0.738	0.18	0.775	3.394	17.14	12.53	28.01
YFR032C	−130	1.13	0.725	0.604	0.657	12.1	20.47	14.35	6.006
YHR185C	−150	0.579012	0.79	0.571	0.919	7.92	15.91	11.5	6.221
YDL186w	−160	1	0.907	0.537	1.082	3.581	9.737	6.778	5.989
YDR065w	−110	1.17	0.638	0.572	0.94	3.415	8.346	7.332	5.056
YER085c	−90	1	0.704	0.761	0.8	3.424	10.02	8.983	5.976
YDL114w	−350	0.7137	0.723	0.567	0.732	3.305	10.78	7.282	9.857
YOL015W	−110	0.5162	0.538	0.375	0.551	7.373	30.36	19.75	20.38
YDR371W	−80	0.9492	0.844	1.269	0.979	3.934	14.14	15.64	20.54
YDR042C	−220	1.17	0.992	0.683	0.945	3.778	11.99	9.581	12.34
YGR273C	−410	0.725172	1.04	0.514	0.764	5.664	31.41	20.3	38.05
YOL024W	−100	0.7137	0.886	0.633	1.006	5.206	15.19	9.306	17.22
YDR218C	−90	1.17	0.741	0.857	1.013	12.06	38.72	22.89	60.56
YJL037W	−270	1.17	1.07	0.76	0.98	9.168	22.85	14.6	40.65
YNL033W	−200	0.599508	0.854	0.92	1.027	4.484	14.28	6.958	19.46
YDR317W	−150	1.17	0.873	0.869	0.663	6.788	16.3	13.39	21.43
YLR343W	−150	0.6903	0.84	0.883	0.733	8.492	24.39	16.58	41.74
YNL318C	−120	0.6903	0.697	0.683	0.731	8.678	25.47	22.36	36.15
YMR017W	−340	0.8424	0.816	0.877	0.838	5.582	19.65	15.07	32.55
YNL019C	−200	0.599508	0.673	0.878	0.933	5.235	16.58	10.11	15.68
YLR308W	−160	1	0.861	1.164	0.863	13.83	25.89	17.35	38.45
YDR260C	−900	0.724104	1.009	1.081	1.075	3.207	9.433	4.805	5.78
YML119W	−160	0.9828	0.928	0.886	1.071	4.886	15.09	9.413	6.545
YLR307W	−120	0.9828	0.771	0.853	1.151	9.16	19.16	14.61	11.32
YPR027C	−250	0.9492	0.811	0.793	0.918	4.635	8.003	6.307	7.148
YEL023c	−520	0.6667	0.755	0.574	1.193	17.78	34.12	8.509	62.09
YFR023W	−230	1.17	0.691	0.575	0.78	17.33	21.26	25.76	54.45
YPL130W	−160	1.13	0.53	0.496	0.895	12.5	20.65	11.66	28
YOR313C	−200	1.13	0.811	0.848	1.085	32.76	20.3	15.71	47.71
YER106w	−156	1.17	0.739	0.451	0.79	9.869	14.58	14.64	5.726
YOR298W	−120	1.17	0.525	0.316	1.066	3.15	10.07	7.816	4.526
YAL018C	−180	1	0.718	0.582	0.592	13.22	25.2	10.17	21.86
YBR250W	−185	1.17	0.895	0.699	0.963	7.33	9.702	3.808	6.169
YJR119C	−190	0.8424	0.759	0.669	0.887	3.024	9.484	7.906	5.538
YGL116W	−86	1.17	0.884	1.424	1.166	5.669	27.1	14.72	22.09
YJL160C	−210	1	0.84	1.229	1.036	5.184	17.08	10.97	26.36
YOL047C	−120	1.13	1.029	1.198	0.922	6.203	13.87	7.925	13.85
YFL012W	−160	1.17	0.835	1.069	1.032	3.316	5.406	6.096	6.138
YOR365C	−130	0.97	0.719	0.893	0.839	4.296	9.187	10.38	13.87
YGL170C	−120	1.17	0.761	0.461	0.902	12.08	28.59	20.9	44.8
YHR184W	−90	1.17	0.836	0.48	0.828	23.33	42.59	28.61	46.02
YHR124W	−220	1.17	0.912	0.641	0.582	9.019	24.16	18.2	25.73
YGL138C	−150	1	1.061	0.622	0.729	8.813	25.39	13.98	30.78
YLR341W	−150	1	0.984	0.663	0.973	8.465	28.8	14.07	37.86
YGR059W	−285	1.17	0.908	0.734	0.84	15.3	31.82	29.84	46.53
YGL015C	−120	0.89	0.816	0.785	0.858	6.785	14.48	11.05	19.09
YNL128W	−150	1.13	0.879	0.869	0.88	6.592	14.6	10.2	21.21
YOL132W	−110	0.97	0.757	0.862	0.689	9.888	36.34	22.09	46.12
YPL021W	−275	0.9492	0.832	1.03	0.906	6.802	16.65	14.25	25.78

(Continued)

Table A1 | Continued

ORF	Position	PWM score	*t*0	*t*0.5	*t*2	*t*5	*t*7	*t*9	*t*11.5
YNL204C	−95	1	0.817	1.021	0.727	9.11	20.96	13.15	19.52
YPR078C	−200	1	0.775	0.83	0.597	10.22	21.85	10.67	24.12
YOR190W	−200	0.749736	0.807	0.643	0.77	4.394	20.05	17.58	28.51
YOR242C	−220	0.603954	0.84	0.76	0.772	5.091	20.51	12.33	33.93
YBR285W	−220	0.6786	1.259	2.197	0.955	1.311	4.261	4.408	3.632
YER100w	−180	0.579852	0.91	0.959	0.91	0.907	2.473	2.403	1.679
YFL024C	−370	0.9492	0.934	0.982	0.899	0.953	1.983	1.428	1.492
YKR019C	−290	1	0.759	1.423	1.21	1.761	5.916	4.075	3.305
YDL103C	−80	0.6786	1.106	1.13	2.457	3.24	6.293	7.124	7.375
YKL042W	−130	0.8424	1.11	1.028	1.684	4.075	5.066	9.726	14.7
YDR516C	−290	0.6786	0.825	0.833	0.375	1.762	7.44	7.489	18.86
YBR180W	−140	0.7137	1.118	0.753	0.825	1.679	3.822	3.977	4.057
YGL162W	−440	0.9492	1.079	0.615	0.629	2.384	8.46	9.129	7.724
YBL079W	−210	0.89	0.867	0.93	0.868	1.044	1.61	1.47	1.505
YGL003C	−940	0.497016	0.851	1.044	0.671	1.508	4.659	3.879	3.94
YFL040W	−120	1	0.849	0.929	0.81	2.22	8.651	6.16	7.922
YDR281C	−260	1.17	0.773	0.95	0.873	1.474	2.908	2.524	2.347
YKR031C	−970	0.874692	0.972	1.195	0.969	1.776	3.156	2.685	2.777
YCL048W	−100	1	1.037	0.882	0.849	2.105	5.175	6.924	8.885
YKL189W	−270	0.9828	0.984	1.058	0.699	2.842	8.395	8.276	11.78
YOR339C	−110	1.17	0.66	0.938	0.66	2.818	6.399	7.83	9.111
YER115c	−270	0.8424	0.893	0.851	1.303	4.93	19.18	14.16	27.39
YGL230C	−200	1	0.879	0.85	0.997	2.96	7.934	7.007	11.31
YOR214C	−240	1.17	0.99	0.753	1.511	2.94	10.17	8.95	16.39
YCR054C	−100	0.6903	0.862	0.599	0.708	1.085	2.989	1.94	2.469
YGR109C	−390	0.9492	0.942	0.754	1.168	2.41	18.01	6.301	18.42
YIR013C	−160	0.97	0.898	0.765	0.685	2.155	17.98	5.302	23.31
YNR034W	−215	0.97	0.875	0.696	0.9	1.613	11.27	10.11	25.48
YDR147W	−90	0.97	0.894	0.63	0.972	2.13	4.719	3.795	3.775
YER105c	−160	1.17	0.782	0.701	0.903	1.376	2.355	1.998	1.96
YER123w	−250	1.17	1.031	0.655	0.854	2.708	5.658	3.827	4.662
YOR297C	−155	1.17	0.813	0.724	1.005	2.462	4.483	3.337	2.762
YDR273W	−130	1	0.785	1.019	1.332	10.35	17.64	15.01	22.09
YBR148W	−230	0.9828	0.81	1.058	1.273	12.24	31.58	12.95	18.16
YOL091W	−110	1	0.716	0.863	1.268	23.86	35.63	20.94	18.92
YPL033C	−80	0.59	0.702	1.038	1.443	12.08	20.52	11.89	13.9
YMR232W	−70	0.6408	0.787	1.197	1.27	3.004	7.303	5.206	6.215
YIL104C	−500	0.8136	0.855	0.608	0.76	0.955	1.918	1.934	1.641
YER168c	0	0.8424	1.125	0.63	0.741	1.138	1.995	1.826	1.803
YKL096W	−250	1.13	1.001	0.27	0.235	1.449	7.336	5.276	5.502
YOR338W	−160	1.13	0.979	0.263	0.399	2.107	3.99	2.855	2.927
YKL171W	−200	0.749736	0.891	0.8	0.766	1.252	1.886	1.472	1.289
YNL121C	−120	0.9828	0.811	0.584	0.521	1.238	2.91	2.066	1.642
YMR252C	−165	1.17	0.737	0.779	2.045	1.544	2.281	3.069	2.112
YPL026C	−5	0.8424	0.95	0.764	1.401	1.77	2.208	1.837	1.819
YMR001C	−300	1.17	0.79	2.314	2.194	13.99	27.04	14.12	21.87
YDL239c	−90	0.874692	0.754	2.022	3.434	10.08	27.01	19.85	16.47
YOR033C	−955	0.749736	0.831	1.791	2.556	9.12	14.95	16.02	15.48
YJR036C	−240	0.84	0.896	2.749	2.642	6.482	13.07	13.31	16.57
YIL144W	−200	1	1.022	3.046	3.225	8.412	11.08	7.961	10.03
YMR198W	−100	0.97	0.729	3.509	5.878	4.756	12.52	7.767	6.062
YOR177C	−230	0.8424	0.828	3.658	3.208	5.039	8.42	7.585	5.789

(Continued)

Table A1 | Continued

ORF	Position	PWM score	*t*0	*t*0.5	*t*2	*t*5	*t*7	*t*9	*t*11.5
YKR034W	−380	0.7137	0.879	7.614	7.731	2.533	3.392	2.375	3.831
YNL202W	−190	1	0.914	3.068	2.073	1.493	2.572	2.466	3.039
YBR069C	−140	1.13	1.186	0.897	0.221	0.563	1.621	2.166	2.715
YGL181W	−100	0.72	1.371	1.425	0.699	0.834	1.294	1.77	1.45
YFL023W	−280	0.9492	0.959	0.81	0.784	0.772	1.065	1.291	1.619
YNL217W	−210	0.6984	0.806	0.513	0.382	0.612	1.861	1.923	1.555
YHR019C	−190	0.5499	0.797	0.477	0.451	0.479	0.743	0.586	0.554
YAL034AW	−200	0.749736	1.08	0.577	0.997	1.021	1.211	1.564	1.263
YDL207w	−140	0.61	0.821	0.489	0.825	0.608	0.717	1.004	0.921
YIL091C	−370	0.6893	0.999	0.452	0.503	0.613	0.632	0.966	0.822
YNL119W	−660	1.0413	0.889	0.17	0.26	0.242	0.275	0.396	0.618
YML106W	−30	0.8424	0.885	0.51	0.705	0.681	0.575	0.863	0.833
YNR053C	−180	0.3948	0.905	0.084	0.318	0.55	0.351	0.588	0.584
YEL015w	−360	1.13	0.906	0.689	0.939	0.834	0.866	0.668	0.682
YER122c	−210	1.17	1	0.769	1.058	0.85	0.85	0.768	0.77
YMR011W	−530	0.6554	0.862	0.177	0.861	0.961	0.488	0.511	0.551
YDL102W	−300	1.17	1.035	1.04	1.39	1.179	1.238	1.187	1.164
YFL014W	−400	0.97	1.343	0.75	3.633	2.061	2.062	1.69	3.541
YOR166C	−250	0.5723	0.886	0.753	1.128	0.969	1.121	0.83	1.038
YDR055w	−380	0.844788	0.794	0.447	0.251	0.211	0.139	0.194	0.143
YKL060C	−200	0.58	1.189	0.283	0.561	0.189	0.14	0.106	0.187
YGR060W	−380	0.97	1.049	0.901	1.429	1.065	0.855	0.695	0.579
YKL126W	−780	0.6893	0.913	1.093	1.038	0.927	0.899	0.579	0.582
YIL160C	−345	1.17	1.007	3.977	1.962	0.841	0.942	1.444	2.791
YLL023C	−200	0.8424	1.063	0.964	0.863	0.486	0.385	0.512	1.007
YOL139C	−80	0.599508	0.899	0.646	0.854	0.63	0.547	0.787	0.869
YIL107C	−90	0.97	0.829	1.421	1.288	1.181	1.203	0.936	0.989
YJL149W	−120	0.603954	0.725	1.567	1.167	1.711	1.648	1.026	0.785
YMR145C	−220	0.8148	0.857	1.167	0.858	0.755	0.957	0.727	0.587
YJL099W	−200	0.6786	0.646	0.785	0.698	1.12	1.625	1.585	0.865
YJR039W	−310	0.84	0.956	1.121	1.058	1.224	1.311	1.657	1.057
YJR025C	−140	0.89	0.667	1.008	0.792	0.886	1.578	1.115	0.722
YER125w	−200	0.6786	0.87	1.34	1.696	1.753	1.459	1.823	1.388
YOR373W	−200	0.5499	0.823	1.109	1.454	1.111	1.257	1.354	1.097
YER099c	−330	0.579852	0.928	1.198	0.942	0.993	1.285	1.094	1.383
YNL317W	−170	0.6903	0.921	1.129	0.812	0.869	1.21	1.05	1.279
YGL002W	−190	0.6786	0.875	1.5	1.328	1.15	2.07	1.89	1.656
YER155c	−30	1.17	0.819	0.988	0.745	0.964	1.255	1.273	1.267
YPR035W	−80	0.3422	0.777	1.049	0.922	0.854	1.562	2.001	2.087
YIL155C	−100	0.6667	0.534	0.622	0.662	0.617	0.962	0.693	0.842
YLL032C	−180	0.724104	0.676	0.656	0.693	0.76	0.876	0.809	0.828
YOR161C	−340	0.9492	0.719	1.248	1.138	1.599	2.601	2.162	2.214
YKR020W	−150	0.84	0.758	0.784	0.893	0.61	1	0.816	0.772

Column 1: Known and predicted target genes of Ndt80 (Jolly et al., 2005).

Column 2: The approximate positions of the potential Ndt80 binding sites used in this analysis. Potential Ndt80 binding sites were identified using the YEASTRACT database (Teixeira et al., 2006), which searched DNA from −1000 to −1 of the target genes for the sequence CRCAAA (Jolly et al., 2005). The position of the site with the highest PWM score is listed.

Column 3: PWM scores (Jolly et al., 2005) of the potential Ndt80 binding sites. A 9-bp-long DNA centering around the CRCAAA core sequence (Jolly et al., 2005) was used to compute a PWM score.

Columns 4–10: mRNA expression levels from 0, 0.5, 2, 5, 7, 9, 11.5 h after the initiation of sporulation (Chu et al., 1998). Expression was calculated as the ratio of red signal divided by green signal, after background subtraction.

Table A2 | Phosphorylation of Cdk1 substrates.

Peptides	Cln	Cln-sum	*P*-score
YCR088W ABP1 165 PPVKKSFT#PSKSPAP -3.06 1.68 0.95	121.3	648	1.4
YCR088W ABP1 169 KSFTPSKS#PAPVSKK -3.06 0.63 0.95	121.3		
YCR088W ABP1 181 SKKEPVKT#PSPAPAA -1.74 0.61 0.95	54.4		
YCR088W ABP1 183 KEPVKTPS#PAPAAKI -1.32 0.63 0.95	309.8		
YCR088W ABP1 313 KGFRNEKS#PAQLWAE -1.18 2.75 0.95	41.2		
YLR131C ACE2 486 IPGSSNNT#PIKNSLP -3.51 1.76 2.72	40.2	471.6	2.5
YLR131C ACE2 501 QKHVFQHT#PVKAPPK -3.46 1.49 2.72	18.2		
YLR131C ACE2 392 SPGGLSIS#PRINGNS -3.28 0.78 2.72	34.9		
YLR131C ACE2 385 FRLFEKTS#PGGLSIS -3.20 0.63 2.72	22.8		
YLR131C ACE2 303 SNTSINGS#PSRKYHR -2.64 0.90 2.72	9.2		
YLR131C ACE2 428 FTPRTQLS#PIHKKRE -2.48 0.86 2.72	125.1		
YLR131C ACE2 259 GSPVILKT#PAMQNGR -2.24 0.83 2.72	13.6		
YLR131C ACE2 564 SPTLHSTS#PLPDEII -2.07 0.56 2.72	20.8		
YLR131C ACE2 80 LDIPLVPS#PKTGDGS -1.27 0.77 2.72	34.7		
YLR131C ACE2 253 NSNSKPGS#PVILKTP -1.06 0.78 2.72	152.1		
YJR083C ACF4 49 SKSPRVTT#PLKPKRL -3.10 0.65 0.69	157.7	269.6	4
YJR083C ACF4 62 RLAIPISS#PQRSTTN -3.04 0.91 0.69	50		
YJR083C ACF4 71 QRSTTNQS#PVSDHAS -1.38 1.00 0.69	61.9		
YDR216W ADR1 188 ASSVKFQT#PTYGTPD -2.07 0.60 0.53	0	0	−10
YBR059C AKL1 504 DPTISEQS#PRLNTQS -2.86 0.60 1.40	95.2		
YBR059C AKL1 801 EALLIELS#PLKEDAG -1.54 0.87 1.40	47.1		
YJL122W ALB1 80 TLQNASSS#PASITTR -1.67 0.56 0.43	7.4		
YOL130W ALR1 143 YVESNIHT#PPKDVGV -2.07 0.51 0.43	28.7		
YOL130W ALR1 188 VRKSSLVS#PVLEIPH -1.45 0.61 0.43	33.3		
YKR021W ALY1 573 VLSSPVLS#PNVQKMN -1.42 1.19 1.48	0		
YJL084C ALY2 213 NGPSRNLS#PINLLKR -2.27 1.68 1.65	61.6	78.6	3.4
YJL084C ALY2 176 GLSSLNLS#PLGAPGN -1.56 0.81 1.65	17		
YKL185W ASH1 253 TRSSKFHS#PSKESFD -1.23 0.60 1.79	30.9	101.4	2.6
YKL185W ASH1 452 RPKAYTPS#PRSPNYH -1.00 1.19 1.79	23.5		
YKL185W ASH1 450 PVRPKAYT#PSPRSPN -1.00 0.96 1.79	23.5		
YKL185W ASH1 455 AYTPSPRS#PNYHRFA -1.00 0.88 1.79	23.5		
YKL052C ASK1 250 NSNNIESS#PLKQGHH -2.34 1.21 0.43	9.1	9.1	0.8
YGR097W ASK10 808 GFRSKVNT#PAIDDYG -2.47 1.29 0.81	0		
YDL088C ASM4 464 SSPIVANS#PNKRLDV -1.08 0.61 0.68	8.8	8.8	1.8
YMR068W AVO2 315 VKTPVGVS#PKKELVS -2.29 0.91 1.47	38.2		
YBR068C BAP2 16 SSGKKETS#PDSISIR -1.11 0.60 0.43	283		
YJL020C BBC1 103 KDLPEPIS#PETKKET -1.03 0.51 1.10	98.8		
YJL095W BCK1 816 PKPPANTS#PQRTLST -2.73 0.83 1.95	18.8	139.7	−10
YJL095W BCK1 747 PKMVFKTS#PKLELNL -1.36 0.84 1.95	98.5		
YJL095W BCK1 411 HYETNVSS#PLKQSSL -1.33 0.89 1.95	22.4		
YER167W BCK2 418 SSMSNRYS#PIRVASP -1.08 1.18 0.83	8.6	8.6	3.6
YIL033C BCY1 89 RSSVMFKS#PFVNEDP -1.19 1.71 0.43	8.1	8.1	0.5
YER155C BEM2 1038 MLINNPAT#PNQKMRD -1.47 0.70 1.11	11.7		
YPL115C BEM3 324 ENKALGFS#PASKEKL -2.66 1.25 2.84	9.3	45.9	3.8
YPL115C BEM3 254 VINNHLHS#PLKASTS -2.50 0.91 2.84	36.6		
YOR198C BFR1 336 ADDLVLVT#PKKDDFV -1.42 0.65 0.43	141.2		
YFL007W BLM10 11 NNDDDIKS#PIPITNK -3.50 1.28 0.43	0		
YFL007W BLM10 29 QLKRFERS#PGRPSSS -1.95 0.76 0.43	28.8		
YNL233W BNI4 410 LRKNHDDT#PVKIDHV -2.64 0.51 2.48	163.6	163.6	−10
YBL085W BOI1 540 FNRISMLS#PVKSSFD -4.26 0.88 2.67	28.3	40.2	1.4
YBL085W BOI1 405 PKPPSYPS#PVQPPQS -3.02 2.23 2.67	5.95		
YBL085W BOI1 412 SPVQPPQS#PSFNNRY -3.02 1.21 2.67	5.95		

(Continued)

Table A2 | Continued

Peptides	Cln	Cln-sum	*P*-score
YER114C BOI2 652 KKSSFMLS#PFRQQFT -4.07 1.68 2.79	32.3	163.4	−10
YER114C BOI2 450 PKPPSYPS#PAQPPKS -1.78 1.18 2.79	2.55		
YER114C BOI2 457 SPAQPPKS#PLLNNTR -1.78 1.05 2.79	2.55		
YER114C BOI2 519 QGGGKALS#PIPSPTR -1.07 0.73 2.79	63		
YER114C BOI2 523 KALSPIPS#PTRNSVR -1.07 0.65 2.79	63		
YHR036W BRL1 56 PHFPSSPS#PLRNTLD -2.12 1.89 1.39	6.4		
YPR171W BSP1 296 QLKPTTLS#PTMKNKP -1.14 0.76 0.77	44.9	136.2	2.8
YPR171W BSP1 309 KPKPTPPS#PPAKRIP -1.10 0.63 0.77	67.9		
YPR171W BSP1 39 KPAGEALS#PVRSHNS -1.08 0.63 0.77	6.1		
YPR171W BSP1 79 YNYEMTFS#PKKTHYS -1.07 0.94 0.77	17.3		
YKL092C BUD2 1066 GNLGNRFS#PTKLSRI -2.17 0.65 0.43	80		
YCL014W BUD3 1515 NAQKVQES#PSGPLIY -1.86 0.75 0.90	30.6	196.6	2
YCL014W BUD3 1440 PVEELPNT#PRSINVT -1.78 0.61 0.90	9.3		
YCL014W BUD3 1549 KDEPIWVS#PSKIDFA -1.62 1.21 0.90	156.7		
YJR092W BUD4 167 PLLSYPES#PIHRSSI -1.55 0.65 1.81	25.9	25.9	5.8
YLR319C BUD6 327 IDDVSKAS#PLAKTPL -1.17 0.61 0.66	71.2	71.2	2.1
YLR353W BUD8 413 YEGHKTPS#PLTKMNK -3.22 0.80 0.49	18.2	36.4	0.7
YLR353W BUD8 411 SRYEGHKT#PSPLTKM -3.22 0.63 0.49	18.2		
YDL099W BUG1 277 AARNTTAT#PIQFADF -1.06 0.92 0.43	0		
YKL005C BYE1 177 DVFLDEES#PRKRKRS -1.36 0.93 1.39	15.7		
YNL278W CAF120 556 FASSVNDS#PSDRAKS -2.42 0.79 2.23	32.6	65.3	5.3
YNL278W CAF120 510 SPSIKRKS#PPLVISE -2.02 0.88 2.23	4.6		
YNL278W CAF120 518 PPLVISES#PHKVHTP -2.02 0.70 2.23	4.6		
YNL278W CAF120 871 VQPANINS#PNKMYGA -1.24 0.61 2.23	0		
YNL278W CAF120 577 NNDRKATT#PEKFERG -1.11 0.95 2.23	23.5		
YNL161W CBK1 93 PALNYPAT#PPPHNNY -1.99 2.09 0.52	0		
YNL161W CBK1 109 ASNQMINT#PPPSMGG -1.99 0.65 0.52	0		
YFR028C CDC14 429 SSAVPQTS#PGQPRKG -1.42 3.07 1.45	0		
YAL038W CDC19 407 VLSTSGTT#PRLVSKY -1.89 1.23 0.43	0		
YLR314C CDC3 503 ELSINSAS#PNVNHSP -2.24 0.63 0.43	557.4		
YLR314C CDC3 509 ASPNVNHS#PVPTKKK -1.67 1.25 0.43	195.5		
YMR001C CDC5 70 KLSALCKT#PPSLIKT -2.83 2.04 0.43	185.2	185.2	3.2
YPR019W CDC54 69 IRAAIGSS#PLNFPSS -1.07 2.46 0.64	0	0	1.9
YJL194W CDC6 368 NSAQVPLT#PTTSPVK -2.53 0.65 1.34	4.25	8.5	−10
YJL194W CDC6 372 VPLTPTTS#PVKKSYP -2.53 0.65 1.34	4.25		
YPL160W CDC60 142 EEEIKEET#PAEKDHE -1.52 0.63 0.43	142		
YGL003C CDH1 227 SQFFDSMS#PVRPDSK -3.18 2.91 2.53	33.7	337	4.1
YBR038W CHS2 86 YRDSAHNS#PVAPNRY -3.58 1.08 0.43	633.6	1106.2	4.7
YBR038W CHS2 60 VFQGLPAS#PSRAALR -2.61 1.08 0.43	26.4		
YBR038W CHS2 133 PVDPYHLS#PQQQPSN -2.57 0.65 0.43	0		
YBR038W CHS2 100 YAANLQES#PKRAGEA -1.53 1.46 0.43	446.2		
YNL298W CLA4 445 PRYAQNSS#PTAAHFQ -1.18 0.73 1.19	30.8		
YNL225C CNM67 121 VPNFIHST#PRENSSK -1.16 0.65 0.43	31.8		
YPR030W CSR2 963 EATSVSAS#PRSSVSY -1.07 1.02 0.85	22.1	22.1	4.7
YOR042W CUE5 364 AETTYIDT#PDTETKK -1.68 1.44 0.43	74.8		
YIR023W DAL81 867 SQSSPNVT#PSHMSRH -1.47 0.94 1.28	13.2	13.2	3.7
YGR092W DBF2 53 AGINDSPS#PVKPSFF -1.70 2.66 0.81	10.8	32.5	3.2
YGR092W DBF2 51 RPAGINDS#PSPVKPS -1.70 1.08 0.81	10.8		
YGR092W DBF2 83 PDMDVSNS#PKKLPPK -1.70 0.84 0.81	10.8		
YDR052C DBF4 11 PTKMIIRS#PLKETDT -3.93 1.38 0.43	31.2	31.2	4.7
YHR164C DNA2 237 KFSDLPSS#PIKAPNV -1.57 0.65 0.73	8.8	8.8	5.2
YER088C DOT6 487 SSDADMLS#PTHSPQK -2.06 0.93 1.80	38.45		

(Continued)

Table A2 | Continued

Peptides	Cln	Cln-sum	*P*-score
YER088C DOT6 491 DMLSPTHS#PQKTLSK -2.00 0.95 1.80	38.45		
YBL101C ECM21 1028 NLDKLLST#PSPVNRS -1.89 0.96 1.07	0	31.7	1.8
YBL101C ECM21 1030 DKLLSTPS#PVNRSHN -1.89 0.91 1.07	13.2		
YBL101C ECM21 33 KGQPFQPS#PTKKLGS -1.58 0.65 1.07	18.5		
YJL201W ECM25 422 TPVALQNT#PVLKPKS -1.38 0.95 0.69	0	0	0.1
YJL201W ECM25 411 SPQRSVTS#PTYTPVA -1.38 0.75 0.69	0		
YBL047C EDE1 238 VNQPNRTT#PLSANST -1.81 0.67 1.80	15.6	15.6	1.1
YNL230C ELA1 235 QAGGQSSS#PKKGPLS -1.03 0.61 0.43	0	0	−10
YMR219W ESC1 1145 DRSNIFSS#PIRVIGA -1.69 0.63 0.43	4	4	−10
YBR102C EXO84 31 AKQKTPPS#PAKPKQK -1.82 0.92 0.43	24.15	48.3	2.3
YBR102C EXO84 28 SSPAKQKT#PPSPAKP -1.82 0.61 0.43	24.15		
YFR019W FAB1 183 MQNSYART#PDSDHDD -1.15 0.70 0.49	6.6		
YJL157C FAR1 15 SFEKKIHT#PPSGDRD -2.05 1.35 1.03	9.5	38.6	2.8
YJL157C FAR1 8 MKT#PTRVSFE -1.38 1.20 1.03	29.1		
YDR130C FIN1 74 VTPRRIMS#PECLKGY -3.11 1.08 0.88	22.5	33	3.7
YDR130C FIN1 36 VFVRLSMS#PLRTTSQ -2.23 1.19 0.88	10.5		
YER032W FIR1 375 PDLEHMKS#PPSTGLN -2.40 0.77 1.05	7.8	23	3.8
YER032W FIR1 84 PNEISQDS#PLKIVFP -2.05 0.93 1.05	6.1		
YER032W FIR1 225 NLYLTPES#PLNRYHL -1.52 1.02 1.05	0		
YER032W FIR1 399 EPSEEPTS#PTRQVNP -1.46 0.60 1.05	9.1		
YNL068C FKH2 708 GSANRARS#PLHSNSN -1.69 1.94 2.34	14.7	35.1	4.4
YNL068C FKH2 833 ETKDINSS#PLKNQGG -1.51 0.60 2.34	20.4		
YPL221W FLC1 714 SPDRASSS#PNSKSYP -1.10 0.84 0.43	29.4		
YAL035W FUN12 386 AKSTPAAT#PAATPTP -1.07 0.63 0.43	21.2		
YAL034C FUN19 211 RLPSPLAS#PNLNRQA -2.52 0.65 1.38	0	0	−10
YAL034C FUN19 207 SSSSRLPS#PLASPNL -2.52 0.65 1.38	0		
YOR178C GAC1 66 KSEIFCTS#PEKNVRF -1.70 0.64 1.49	63.8	63.8	2.5
YOL051W GAL11 163 QQQRRQLT#PQQQQLV -1.24 0.74 1.37	8.7		
YPL248C GAL4 703 SPGSVGPS#PVPLKSG -1.02 0.65 0.62	11.9	11.9	−10
YDL226C GCS1 170 LENRRSAT#PANSSNG -4.40 1.11 0.43	6.4		
YDL226C GCS1 161 VAQSREGT#PLENRRS -1.32 1.89 0.43	170.9		
YMR255W GFD1 111 EISPPPVS#PSKMKTT -1.87 0.65 0.44	44		
YMR255W GFD1 106 SQKATEIS#PPPVSPS -1.43 0.60 0.44	0		
YDR309C GIC2 337 AFFPSRQS#PLPKRRN -3.37 0.79 0.85	17.2		
YDR507C GIN4 462 IVNQSSPT#PASRNKR -3.48 0.65 0.43	16.5	44.1	3.9
YDR507C GIN4 435 ASSSNLTT#PGSSKRL -2.46 0.76 0.43	8.1		
YDR507C GIN4 460 STIVNQSS#PTPASRN -1.74 0.87 0.43	19.5		
YER054C GIP2 213 GVQARDGS#PMLIRSK -1.18 0.65 1.26	38.1		
YAL031C GIP4 520 ETKKSVVS#PEKRKLI -1.00 0.65 0.69	44.9		
YDR096W GIS1 696 ISREASKS#PISSFVN -2.86 0.60 0.99	29		
YDR096W GIS1 425 TTISRISS#PLLSRMM -1.43 0.73 0.99	9.2		
YLR258W GSY2 655 RPLSVPGS#PRDLRSN -1.65 2.96 0.43	528.1		
YMR192W GYL1 17 ERIEVPRT#PHQTQPE -2.35 0.76 0.57	18		
YOR070C GYP1 546 TPTKDFQS#PTTALSN -3.64 0.84 0.78	9.15	28	−10
YOR070C GYP1 539 PRVASFVT#PTKDFQS -3.64 0.84 0.78	9.15		
YOR070C GYP1 555 TTALSNMT#PNNAVED -2.71 0.60 0.78	9.7		
YDL234C GYP7 265 DSWLTNNS#PIQKSQI -1.18 0.56 0.43	0		
YJL165C HAL5 64 IITSNVSS#PSISPVH -1.58 0.80 0.46	0	0	1.4
YOR358W HAP5 8 MTDRNFS#PQQGQGP -1.03 0.72 0.43	7.8		
YDL223C HBT1 671 KQDEDPLS#PRQTTNR -1.35 0.56 0.43	22.7		
YDR458C HEH2 123 MQIQEEKS#PKKKRKK -1.53 1.97 1.70	156.1		
YIL112W HOS4 690 KKREKTQS#PILASRR -3.73 0.65 1.48	29.6	43.7	3.4

(Continued)

Table A2 | Continued

Peptides	Cln	Cln-sum	*P*-score
YIL112W HOS4 290 NLSNMNSS#PAQNPKR -2.89 0.79 1.48	14.1		
YOL123W HRP1 462 TSNTDSGS#PPLNLPN -1.02 0.91 0.43	0		
YKL101W HSL1 1220 ILSKLRLS#PENPSNT -2.90 1.08 0.54	22.8	22.8	0.7
YHR094C HXT1 31 GRSKAMNT#PEGKNES -2.04 0.67 0.43	6	6	0.6
YJL146W IDS2 130 PEPSERAS#PIRQPSV -1.10 0.65 0.43	8.8		
YHR132W-A IGO2 128 SSGPPPRS#PNK -2.83 1.27 0.43	566.3		
YNL106C INP52 1016 EISIVSVS#PRKGESN -4.31 0.81 0.43	22.45	44.9	−10
YNL106C INP52 1005 EPSSKLLS#PTKEISI -4.31 0.59 0.43	22.45		
YOR109W INP53 986 PSTSKEKS#PTPQTST -4.34 0.51 0.43	20.9		
YOR109W INP53 988 TSKEKSPT#PQTSTAS -2.25 1.46 0.43	0		
YPL209C IPL1 76 MESSKIPS#PIRKATS -2.10 1.23 0.68	13	13	2.6
YPL242C IQG1 49 NSSLNIAS#PSHLKTK -5.16 1.10 0.88	52.8	154.4	−10
YPL242C IQG1 365 NKSLSYYS#PTISKYL -3.41 1.13 0.88	15.7		
YPL242C IQG1 354 PTPSLEYS#PIKNKSL -2.71 0.82 0.88	49.5		
YPL242C IQG1 315 NCSDFSNT#PSPYNEA -1.80 0.63 0.88	5.1		
YPL242C IQG1 404 KYSPSHYS#PMRRERM -1.70 1.05 0.88	18.6		
YPL242C IQG1 268 NINTAPAS#PEEPKEK -1.26 0.80 0.88	9.4		
YPL242C IQG1 317 SDFSNTPS#PYNEAPK -1.14 0.67 0.88	3.3		
YBR245C ISW1 694 TSTGSAGT#PEPGSGE -2.32 1.11 0.43	20.3		
YOR304W ISW2 1079 TSATREDT#PLSQNES -3.00 0.74 0.43	43.8		
YPR141C KAR3 21 TQHLSTPS#PKNDILA -2.64 1.01 0.43	51.4	51.4	3.4
YPL269W KAR9 632 TPLSQLLS#PREGRLD -1.11 0.93 0.92	4.5	4.5	0.8
YPL269W KAR9 496 NPFFDPES#PNKGKLI -1.11 0.75 0.92	0		
YHR158C KEL1 613 ANQIKNNS#PILETLP -3.02 2.21 1.64	108.1	175.1	2.1
YHR158C KEL1 503 APLASAPS#PAPKDFS -2.93 0.89 1.64	11.2		
YHR158C KEL1 67 SNVNKTSS#PPMFARK -1.60 1.18 1.64	55.8		
YHR158C KEL1 689 GVAQMASS#PSKDQFK -1.16 0.87 1.64	0		
YHR102W KIC1 735 PLFGVGTS#PNRKPAG -2.07 0.74 0.79	9.8	9.8	0.8
YLR096W KIN2 24 TSKGGSLS#PTPEAFN -3.37 1.01 1.31	25.3	81.6	3.6
YLR096W KIN2 609 IPEQAHTS#PTSRKSS -1.59 1.02 1.31	22.8		
YLR096W KIN2 643 EYQQRSAS#PVVGEHQ -1.09 0.86 1.31	33.5		
YOR233W KIN4 460 GLVTIPGS#PTTARTR -2.37 0.77 1.32	38.1		
YKL168C KKQ8 37 PPRSRDSS#PINVTRI -2.07 0.65 0.50	6.6	6.6	−10
YJR070C LIA1 281 EALGAIAS#PEVVDVL -1.28 0.75 0.43	0		
YGL090W LIF1 261 KPISELNS#PGKRMKR -1.98 0.84 0.43	13.1	13.1	−10
YDR439W LRS4 146 KPTIHLLS#PIVNRDK -3.40 0.98 0.43	32.6	58.5	2.3
YDR439W LRS4 230 RLSALQKS#PELRKER -2.94 0.51 0.43	25.9		
YAL024C LTE1 212 YARQSFAS#PDFRNQS -4.00 0.91 2.06	33.6	41	4.6
YAL024C LTE1 614 SEAITNMT#PRRKNHS -2.33 0.81 2.06	7.4		
YDL182W LYS20 396 NFHAEVST#PQVLSAK -1.25 1.22 0.43	119.8		
YDL131W LYS21 410 DFHAELST#PLLKPVN -1.00 1.25 0.43	357.4		
YJL013C MAD3 478 AVKPRQLT#PILEMRE -2.92 0.75 0.55	11.2	11.2	−10
YKL093W MBR1 69 FNFQPDSS#PCNAKCQ -2.59 0.65 0.43	8.9		
YEL032W MCM3 781 QPASNSGS#PIKSTPR -1.90 0.75 0.43	42.6	42.6	3.1
YGL197W MDS3 1387 KSSAFPQS#PIRAYGS -2.90 0.84 1.03	15.8	32.4	−10
YGL197W MDS3 693 EDDEDPVS#PKPVSKS -1.08 0.65 1.03	16.6		
YOR174W MED4 237 QMAKKEGT#PKTDSFI -1.09 0.63 0.43	18.5		
YIL046W MET30 67 KMTMATRS#PSSSPDL -1.27 0.68 0.43	7.2		
YGL035C MIG1 264 QQQQNSLS#PRYSNTV -2.20 0.88 2.24	21.2		
YMR036C MIH1 27 FQKISLKS#PFGKKKN -4.30 0.83 2.16	29.1	29.1	3.9
YNL074C MLF3 297 PATSPYVS#PQQSARQ -2.97 1.18 1.07	12.8		
YNL074C MLF3 79 KNSNNVSS#PLDNVIP -2.18 0.65 1.07	29.8		

(Continued)

Table A2 | Continued

Peptides	Cln	Cln-sum	*P*-score
YNL074C MLF3 56 FYNLQTIS#PIPISGS -1.94 0.65 1.07	5.7		
YNL074C MLF3 265 CPFILKRS#PPQAYSS -1.77 0.56 1.07	37.4		
YNL074C MLF3 183 SSESSPAS#PDLKLSR -1.68 0.65 1.07	5.7		
YNL074C MLF3 180 TLPSSESS#PASPDLK -1.60 0.65 1.07	9.8		
YLL061W MMP1 21 FSTSVLST#PSNEGNN -3.83 0.63 0.43	0		
YLR190W MMR1 37 SFQNLLNS#PTKLKLD -1.11 0.83 0.51	0	0	3.8
YIL106W MOB1 80 ESDHGRMS#PVLTTPK -4.65 0.65 0.44	79.5	143.6	3.8
YIL106W MOB1 36 ANNAGSVS#PTKATPH -1.20 1.07 0.44	64.1		
YFL034C-B MOB2 76 SQQLTSTT#PQSQQQE -1.03 1.02 0.74	0		
YPL082C MOT1 791 SFVSEIFS#PVMNKQL -2.30 0.65 0.43	7.3		
YLR219W MSC3 46 ASAASAAS#PDRTNYS -1.13 0.65 0.63	9.6	9.6	2.1
YDR097C MSH6 228 YNTSHSSS#PFTRNIS -1.84 1.18 0.43	33.1	33.1	5.3
YLR116W MSL5 378 SRYAPSPS#PPASHIS -1.21 1.06 0.71	126.6		
YLR116W MSL5 376 ASSRYAPS#PSPPASH -1.21 0.74 0.71	126.6		
YKL062W MSN4 178 FNENIELS#PHQHATS -1.58 0.79 1.42	2.2		
YKL062W MSN4 161 EQLEKVFS#PMNPIND -1.58 0.65 1.42	2.2		
YAR033W MST28 179 TATSIGNS#PVTAKPE -1.19 0.51 0.43	9.1		
YPL070W MUK1 245 IVGTSVSS#PNKMKTF -2.42 0.99 0.43	15		
YPL070W MUK1 67 ERLENNKS#PILTKQE -1.10 0.73 0.43	32.3		
YLR457C NBP1 253 LKIDLSPS#PIRRTNS -1.04 1.12 0.56	3.45	6.9	3.7
YLR457C NBP1 251 KPLKIDLS#PSPIRRT -1.04 0.94 0.56	3.45		
YBL024W NCL1 426 TEKLSSET#PALESEG -1.76 0.75 0.43	11.7		
YJL076W NET1 676 RNILPQRT#PRSAAKR -4.43 0.84 1.05	354.8	478.8	4.6
YJL076W NET1 1056 TQLMDMSS#PPSVKSK -3.50 1.12 1.05	12.65		
YJL076W NET1 1042 VNKKINAT#PDKIPVT -3.50 1.02 1.05	12.65		
YJL076W NET1 1032 SSKIEAPS#PSVNKKI -3.46 0.56 1.05	44.1		
YJL076W NET1 252 PPPTQPQS#PPIRISS -2.69 1.10 1.05	9.5		
YJL076W NET1 830 SFPVVGGS#PSVATKG -2.49 0.64 1.05	8.3		
YJL076W NET1 447 SIADNNGS#PVKNSPL -2.23 1.18 1.05	9.3		
YJL076W NET1 452 NGSPVKNS#PLGDAMP -2.23 0.91 1.05	9.3		
YJL076W NET1 166 RSKLNNGS#PQSVQPQ -2.13 0.65 1.05	0		
YJL076W NET1 297 QQRLLSGT#PIMSTMT -1.81 1.18 1.05	5.2		
YOR056C NOB1 367 GNRYSVAS#PLSKNSQ -3.14 1.69 0.58	13		
YPR072W NOT5 306 FDNSTLGT#PTTHVSM -1.33 0.97 0.55	38.1		
YML059C NTE1 645 RNAQLSTS#PLSLDNT -1.12 0.66 0.44	0		
YDR001C NTH1 66 MSVFDNVS#PFKKTGF -5.54 0.75 0.43	68.7	68.7	2.4
YOR098C NUP1 767 HNKEKSNS#PTSFFDG -1.13 0.89 1.29	11.8	11.8	5.2
YIL115C NUP159 854 HVKAKSES#PFSAFAT -1.72 1.83 2.37	19.5		
YIL115C NUP159 735 FKFGTQAS#PFSSQLG -1.09 1.13 2.37	0		
YAR002W NUP60 460 VQPDLSVT#PQKSSSK -4.10 0.79 1.02	25.2	239	2.1
YAR002W NUP60 222 FNYSSLPS#PYKTTVY -2.35 1.65 1.02	23		
YAR002W NUP60 382 NVVVAETS#PEKKDGG -1.47 1.22 1.02	153.5		
YAR002W NUP60 312 IRKHKRVS#PNAAPRQ -1.17 0.60 1.02	37.3		
YHR195W NVJ1 298 SLLHIQVS#PTKSSNL -1.06 0.65 0.43	11.4		
YHL029C OCA5 8 MHDKKS#PMANSHY -1.60 0.83 0.58	8.2		
YBR060C ORC2 217 LTLSRNFT#PTPVPKN -1.30 0.87 1.08	8.8	8.8	3.6
YPR162C ORC4 9 TISEARLS#PQVNLLP -1.51 0.56 0.55	0		
YHR118C ORC6 116 KQFAWTPS#PKKNKRS -1.12 1.58 1.30	12.45	24.9	4.1
YHR118C ORC6 114 PMKQFAWT#PSPKKNK -1.12 1.18 1.30	12.45		
YGR178C PBP1 193 ERKLEKWT#PEEGAEH -4.18 1.35 2.14	8.4		
YGR178C PBP1 436 TPSAKTVS#PTTQISA -1.95 0.92 2.14	36.6		
YER149C PEA2 345 PVTWDPSS#PSSVGSP -1.42 1.27 0.60	16.1		

(Continued)

Table A2 | Continued

Peptides	Cln	Cln-sum	*P*-score
YML123C PHO84 579 NNDIESSS#PSQLQHE -1.53 0.65 0.43	45.9		
YLR273C PIG1 645 FRDYFYKS#PSP -2.40 0.63 0.99	0	0	1
YBL051C PIN4 541 LLRNSQIS#PPNSQIP -1.25 1.31 0.89	15.8		
YBL051C PIN4 466 SMQPTLTS#PKMNIHH -1.01 0.79 0.89	53.9		
YIL122W POG1 168 INASELAS#PRGHRRY -2.48 0.93 0.43	42.5	42.5	3.3
YNL102W POL1 215 KYLEIESS#PLKLQSR -2.32 0.83 0.43	7.4	119.5	2.3
YNL102W POL1 313 PFVTAPGT#PIGIKGL -2.02 2.07 0.43	3		
YNL102W POL1 305 SRSNPSTS#PFVTAPG -2.02 0.83 0.43	3		
YNL102W POL1 170 LRENLNSS#PTSEFKS -1.28 0.77 0.43	106.1		
YBL035C POL12 111 FGLSIPKT#PTLKKRK -3.50 2.60 0.65	16.7		
YLR018C POM34 221 YLFKGLET#PLKARQR -1.68 1.18 0.85	9.8		
YLR018C POM34 273 NDNNSPHT#PVTRKGY -1.13 0.65 0.85	76.9		
YIL114C POR2 103 GDVNAFLT#PQSIKNA -3.59 0.88 0.43	0		
YML016C PPZ1 265 AYSTPLNS#PGLSKLT -1.83 1.21 0.65	4.85		
YML016C PPZ1 261 DGNTAYST#PLNSPGL -1.59 1.39 0.65	4.85		
YML016C PPZ1 142 MIQMEPKS#PILKTNN -1.54 2.41 0.65	4.3		
YDR436W PPZ2 299 NVNGRGTS#PIPNLNI -2.54 1.18 0.74	16.6		
YDR436W PPZ2 310 NLNIDKPS#PSASSAS -2.54 0.59 0.74	16.6		
YMR137C PSO2 193 SFISNPSS#PAKTKRD -2.99 0.64 0.43	11.7	11.7	−10
YML017W PSP2 340 TPLSKLDS#PALELQS -1.19 0.75 0.46	0		
YBL046W PSY4 434 TYRENISS#PLGKKSR -2.48 1.02 0.43	23.2		
YBL046W PSY4 347 FTNMDLTT#PKKYKHT -1.83 1.02 0.43	5.3		
YJR059W PTK2 784 NSLRSLGS#PSVSSSK -2.44 0.65 2.12	25	246.8	2.3
YJR059W PTK2 69 GSGSGGNS#PSSSAGA -1.92 0.96 2.12	10.5		
YJR059W PTK2 727 LKSMLNST#PTTPTHN -1.25 0.86 2.12	45		
YJR059W PTK2 730 MLNSTPTT#PTHNGPT -1.25 0.73 2.12	45		
YJR059W PTK2 737 TPTHNGPT#PLPAKAG -1.08 0.65 2.12	121.3		
YER075C PTP3 272 TATTPLSS#PQMNLKL -2.45 0.65 1.14	8.1		
YGR253C PUP2 56 GVEKRATS#PLLESDS -3.33 1.35 0.43	49.2		
YDR217C RAD9 26 AIKEALHS#PLADGDM -1.43 0.63 1.44	11.8	50.2	3.8
YDR217C RAD9 937 KSMTNVLS#PKKHTDD -1.21 0.63 1.44	8.6		
YDR217C RAD9 56 STNIIEGS#PKANPNP -1.15 1.07 1.44	29.8		
YJR033C RAV1 1211 PVQKLLKS#PTKDRAY -1.08 0.63 0.43	83.8	83.8	2.4
YLR248W RCK2 46 DVSQITSS#PKKSFQD -1.26 0.51 0.43	213.2		
YDR195W REF2 245 DDKNSSPS#PTASTSS -1.67 0.61 0.43	37.5		
YDR028C REG1 898 RIVNNTPS#PAEVGAS -1.47 0.74 1.73	0		
YDR028C REG1 896 SFRIVNNT#PSPAEVG -1.47 0.63 1.73	0		
YDR028C REG1 421 NLDQNLNS#PDNNRFP -1.10 0.60 1.73	6.6		
YOR217W RFC1 48 DQESTNKT#PKKMPVS -2.12 0.56 0.43	0		
YOR127W RGA1 278 SRNLLNKT#PLRNSSG -4.58 1.73 1.92	35.2	55.1	3.7
YOR127W RGA1 331 LLTSVLHS#PVSVNMK -3.28 1.27 1.92	14.3		
YOR127W RGA1 291 SGQYLAKS#PSSYRQG -2.53 1.69 1.92	5.6		
YDR379W RGA2 772 GKVPLSPS#PKRLDYT -2.84 0.77 1.92	26.6	123.4	2.3
YDR379W RGA2 763 RVHDELPS#PGKVPLS -2.84 0.65 1.92	26.6		
YDR379W RGA2 770 SPGKVPLS#PSPKRLD -2.84 0.65 1.92	26.6		
YDR379W RGA2 380 SKSMNHVS#PITRTDT -1.48 0.60 1.92	15.2		
YDR379W RGA2 733 DLESQQRS#PNSSSGG -1.34 0.75 1.92	28.4		
YDR137W RGP1 370 SSIIDIDS#PLEDNEF -1.31 0.56 0.83	26.2		
YKL038W RGT1 229 SYNTVQQS#PITNKHT -2.04 1.16 0.96	0	5.3	−10
YKL038W RGT1 469 EASSPGST#PQRSTKK -1.85 1.05 0.96	5.3		
YBR275C RIF1 45 KTNLPPPS#PQAHMHI -1.75 0.63 0.91	0	0	−10
YFL033C RIM15 1565 PTMTKFKS#PLSPANT -1.55 1.30 3.06	4.3	4.3	−10

(Continued)

Table A2 | Continued

Peptides	Cln	Cln-sum	*P*-score
YPR018W RLF2 94 KLLCYKNS#PIQSTKY -2.47 0.83 0.54	46.4	53.9	2.2
YPR018W RLF2 515 QTASQSQS#PEKKQKA -1.54 1.52 0.54	7.5		
YLR371W ROM2 171 DHPLPPMS#PRNEVYQ -1.97 0.79 0.43	10.5	18.6	−10
YLR371W ROM2 216 STGSASTT#PTQARKS -1.10 0.92 0.43	8.1		
YER169W RPH1 575 SLIKRVKS#PNIVTLN -3.39 1.18 1.15	8.3		
YER169W RPH1 561 ISHSAPHS#PVNPNIS -1.38 0.77 1.15	28.7		
YER169W RPH1 430 SKSSGVSS#PLLSRMK -1.08 1.18 1.15	19		
YDR418W RPL12B 38 KIGPLGLS#PKKVGED -2.25 2.73 0.43	411		
YIL153W RRD1 341 IEQANAGS#PGREQTS -2.00 0.60 0.52	7.9	7.9	0.9
YLR357W RSC2 682 IPLSRVGS#PGAGGPL -2.69 1.09 0.94	81.6		
YLR357W RSC2 243 LRDNRSTT#PSHSGTP -1.25 0.73 0.94	11.2		
YOR014W RTS1 242 HSFERLPT#PTKLNPD -3.54 1.45 1.12	17.2	17.2	4.4
YDR159W SAC3 866 SDKNLIFS#PVNDEFN -2.76 0.74 0.87	10	100.4	−10
YDR159W SAC3 600 VKPQINTS#PKRVATR -1.27 0.66 0.87	90.4		
YDR389W SAC7 46 ENITVPRS#PTSLSRN -1.92 0.65 2.11	13.4	121.6	2.1
YDR389W SAC7 16 GSKIENVS#PSKGHVP -1.49 0.80 2.11	108.2		
YER129W SAK1 966 KLSELSNS#PQKGSNN -1.63 0.56 1.41	16.6	25.3	6.4
YER129W SAK1 36 SSSVSLRS#PTKSSAT -1.47 0.65 1.41	8.7		
YER120W SCS2 204 EKQTSNST#PAPQNQI -1.76 0.56 0.43	11.6		
YGL056C SDS23 405 SSSPSPST#PPVTTLP -1.32 0.60 0.92	0		
YBR214W SDS24 458 TAMEDPPS#PRSSAIA -1.30 0.86 0.86	466.8		
YLR166C SEC10 485 NVDAFMHS#PRGNTHS -1.44 0.60 0.43	24.7		
YPL085W SEC16 607 VSVPNIVS#PKPPVVK -2.34 0.76 2.62	12.8	191.6	1.6
YPL085W SEC16 1515 IGDSLQGS#PQRIHNT -1.43 0.65 2.62	178.8		
YDL195W SEC31 836 PSQPSMAS#PFVNKTN -1.23 0.91 1.47	0		
YDL195W SEC31 980 PSSVSMVS#PPPLHKN -1.07 1.23 1.47	15.1		
YDR170C SEC7 1240 DVWGKKAT#PTELAQE -1.37 1.42 0.43	23.5		
YOR057W SGT1 171 NSSHSPIS#PLKIETA -1.37 0.51 0.43	40.5		
YBL058W SHP1 315 GQGQRLGS#PIPGESS -1.29 2.61 0.43	80.5		
YBL058W SHP1 322 SPIPGESS#PAEVPKN -1.05 0.65 0.43	31.4		
YDL225W SHS1 447 SSPKFLNS#PDLPERT -2.11 0.79 0.43	103.7		
YOL004W SIN3 304 DDPIRVTT#PMGTTTV -1.62 2.72 0.58	74.4		
YOL004W SIN3 316 TTVNNNIS#PSGRGTT -1.62 0.56 0.58	74.4		
YDR422C SIP1 200 SSATASPS#PTRSSSV -1.06 0.75 0.43	5.15		
YDR422C SIP1 198 LESSATAS#PSPTRSS -1.06 0.65 0.43	5.15		
YDL042C SIR2 23 NKVSNTVS#PTQDKDA -1.13 0.56 0.43	20.2		
YLR442C SIR3 454 HSMNENPT#PEKGNAK -1.13 0.88 0.64	26.6		
YDR227W SIR4 389 KRMEILKS#PHLSKSP -2.96 0.56 0.53	19.8	38.8	4.8
YDR227W SIR4 342 TSKKIVPS#PKKVAID -2.04 0.51 0.53	19		
YKR072C SIS2 47 GKDSIINS#PVSGRQS -1.70 0.63 1.15	7.3		
YKR072C SIS2 56 VSGRQSIS#PTLSNAT -1.33 0.65 1.15	8.9		
YDR409W SIZ1 139 SPSVIRQS#PTQRRKT -2.41 0.75 1.67	12		
YDR409W SIZ1 132 PPTVQQQS#PSVIRQS -2.41 0.66 1.67	12		
YHR149C SKG6 126 LPTMKDYS#PGINHLY -1.61 0.51 0.43	0		
YHR149C SKG6 232 PDNFSNCT#PIRASSR -1.61 0.60 0.43	4.5		
YNL167C SKO1 113 IISPPILT#PGGSKRL -1.81 1.65 1.31	2.6		
YNL167C SKO1 108 QQRPTIIS#PPILTPG -1.81 1.35 1.31	2.6		
YNL167C SKO1 94 HNDVKKDS#PSFLPGQ -1.43 0.91 1.31	2.7		
YBL007C SLA1 437 IKKNFTKS#PSRSRSR -2.93 0.77 0.74	81.7		
YNL243W SLA2 294 PARTPART#PTPTPPV -1.62 2.12 0.43	325	580.3	1.9
YNL243W SLA2 308 VVAEPAIS#PRPVSQR -1.62 0.70 0.43	85.1		

(Continued)

Table A2 | Continued

Peptides	Cln	Cln-sum	*P*-score
YNL243W SLA2 298 PARTPTPT#PPVVAEP -1.13 0.60 0.43	85.1		
YNL243W SLA2 296 RTPARTPT#PTPPVVA -1.09 1.02 0.43	85.1		
YGL113W SLD3 467 IINSVPSS#PALRRVD -4.42 1.04 0.80	0		
YDR515W SLF1 42 TSPWKSSS#PDSNTVI -1.10 0.63 0.43	57.7		
YBR156C SLI15 268 KVRTVKES#PIAFKKK -3.00 0.81 1.22	16.9	29.3	−10
YBR156C SLI15 144 SIHDTNKS#PVEPLNS -1.04 0.65 1.22	12.4		
YNL047C SLM2 649 FYIENVDS#PRKSNQL -2.33 0.79 0.51	7.4		
YLR086W SMC4 128 RLELLQLS#PVKNSRV -2.92 1.53 0.43	49.9	78.1	4.1
YLR086W SMC4 113 YSQSPPRS#PGRSPTR -1.98 2.01 0.43	14.1		
YLR086W SMC4 117 PPRSPGRS#PTRRLEL -1.98 1.40 0.43	14.1		
YDR006C SOK1 193 NINNPSPS#PPPSSKQ -1.24 0.65 0.43	6.85		
YDR006C SOK1 191 YTNINNPS#PSPPPSS -1.24 0.64 0.43	6.85		
YLL021W SPA2 1087 SPELAKNS#PLAPIKK -5.19 0.60 1.29	53.8	1190	3.4
YLL021W SPA2 585 NDVEEEES#PVKPLKI -3.34 1.18 1.29	453.7		
YLL021W SPA2 646 EDNDKYVS#PIKAVTS -2.55 0.72 1.29	16.9		
YLL021W SPA2 961 TAQESIKS#PEAARKL -2.54 0.51 1.29	96.2		
YLL021W SPA2 274 KGPEQLKS#PEVQRAE -2.09 0.65 1.29	71.3		
YLL021W SPA2 599 ITQKAINS#PIIRPSS -2.04 0.84 1.29	19.2		
YLL021W SPA2 254 NYWDVNDS#PIIKVDK -1.68 0.65 1.29	18.7		
YLL021W SPA2 937 EADSRVES#PGMKEQI -1.58 0.65 1.29	91.4		
YLL021W SPA2 979 GEVDKIES#PRMVRES -1.58 0.76 1.29	322		
YLL021W SPA2 1080 EPNSQIVS#PELAKNS -1.57 0.91 1.29	7.5		
YLL021W SPA2 883 EPLGNVES#PDMTQKV -1.44 0.60 1.29	32.7		
YLL021W SPA2 910 ESDSRVES#PGMTGQI -1.33 0.56 1.29	6.6		
YGL093W SPC105 356 DYAASVTT#PVKEAKD -1.10 0.79 1.43	13.9	13.9	−10
YPL124W SPC29 59 RAQERMSS#PLHRLSP -1.54 0.59 0.43	104	104	1.6
YKL042W SPC42 357 NMSETFAT#PTPNNR -1.23 1.18 0.90	18.6	18.6	0.5
YHR152W SPO12 118 QLQQRFAS#PTDRLVS -5.07 0.93 0.43	29.75	59.5	−10
YHR152W SPO12 125 SPTDRLVS#PCSLKLN -5.07 0.93 0.43	29.75		
YER161C SPT2 173 KRPQKKAS#PGATLRG -1.18 0.77 0.43	0	0	−10
YML034W SRC1 241 LGKLSVKT#PIKNTNR -3.53 1.27 1.61	188.1	188.1	2.9
YML034W SRC1 80 KMDRPSSS#PSIASPR -3.03 0.51 1.61	96.1		
YML034W SRC1 85 SSSPSIAS#PRRSRRA -2.60 0.51 1.61	81.7		
YML034W SRC1 291 ANGTGHST#PLSKLKV -2.19 0.67 1.61	30.1		
YKR091W SRL3 212 RVDNVNVS#PLRWSSH -2.87 0.80 0.83	10.8	10.8	2.3
YCL037C SRO9 40 PAPLPTSS#PWKLAPT -2.84 1.10 0.52	10.5		
YDR293C SSD1 286 QQPQQQLS#PFRHRGS -2.67 1.17 0.43	0	57.5	0.1
YDR293C SSD1 267 KTRNNEYS#PGINSNW -2.52 0.75 0.43	12.6		
YDR293C SSD1 231 RRATSNLS#PPSFKFP -1.30 1.12 0.43	23.8		
YDR293C SSD1 492 NDSDSLSS#PTKSGVR -1.03 0.84 0.43	21.1		
YLR006C SSK1 195 LLRFASVS#PYPKFHS -2.85 0.63 2.57	0	26.4	2.8
YLR006C SSK1 673 TDSVLVKS#PQKPIAP -1.43 0.83 2.57	26.4		
YNR031C SSK2 54 TQARVASS#PISPGLH -2.48 0.91 0.51	45.3		
YNR031C SSK2 57 RVASSPIS#PGLHSTQ -2.48 0.79 0.51	45.3		
YDR443C SSN2 748 NDIPQTES#PLKTVDS -4.10 1.01 1.07	0	0	−10
YNL309W STB1 72 KTLLEAIS#PAKKPLH -5.02 1.13 1.13	47.9	174.9	2.9
YNL309W STB1 89 TNKMTVIS#PVKFVEK -3.35 0.79 1.13	15		
YNL309W STB1 99 KFVEKPNT#PPSSRQR -2.71 1.03 1.13	112		
YFL026W STE2 382 NQFYQLPT#PTSSKNT -1.15 0.92 0.43	17.1		
YHL007C STE20 203 STDIRRAT#PVSTPVI -2.47 0.60 1.11	33	160	−10
YHL007C STE20 562 TPQQVAQS#PKAPAQE -2.28 0.90 1.11	7.1		
YHL007C STE20 502 MNSAANVS#PLKQTHA -1.85 0.65 1.11	27.6		

(Continued)

Table A2 | Continued

Peptides	Cln	Cln-sum	*P*-score
YHL007C STE20 512 KQTHAPTT#PNRTSPN -1.53 0.65 1.11	13.2		
YHL007C STE20 517 PTTPNRTS#PNRSSIS -1.11 0.60 1.11	79.1		
YDR103W STE5 329 SNYTFLHS#PLGHRRI -2.83 0.65 0.96	28.4		
YGR008C STF2 28 HTGNYGES#PNHIKKQ -1.50 1.04 0.43	195.4		
YDL048C STP4 191 TTGFKTIT#PSPPTQH -1.40 0.73 1.17	12.35		
YDL048C STP4 193 GFKTITPS#PPTQHQS -1.40 0.73 1.17	12.35		
YDR310C SUM1 738 QTENTSIS#PKKRRTE -1.71 0.51 0.53	34.1		
YDR310C SUM1 379 KFHQIPSS#PSNPVSQ -1.19 0.65 0.53	0		
YJL187C SWE1 373 DTDEEIST#PTRRKSI -2.17 1.04 2.89	6.6	15.4	4.6
YJL187C SWE1 111 DSRIKRWS#PFHENES -1.58 0.93 2.89	8.8		
YER111C SWI4 806 PSKILENS#PILYRRR -3.48 0.77 1.12	0	13.7	1.9
YER111C SWI4 20 NTNHQNIT#PISKSVL -3.22 0.65 1.12	13.7		
YDR146C SWI5 522 INTYTTNS#PSKITRK -4.00 1.38 2.61	0	365.8	4.7
YDR146C SWI5 492 FVISETPS#PVLKSQS -2.48 1.08 2.61	30.6		
YDR146C SWI5 300 GFNDSLIS#PKKIRSN -2.41 0.80 2.61	7.8		
YDR146C SWI5 261 SNTSFTGS#PSRRNNR -2.14 1.50 2.61	0		
YDR146C SWI5 250 NSLSPMIS#PPMSNTS -2.14 0.71 2.61	0		
YDR146C SWI5 664 GTSSVSSS#PIKENIN -2.08 1.15 2.61	142.1		
YDR146C SWI5 505 QSKYEGRS#PQFGTHI -1.70 1.11 2.61	180.9		
YDR146C SWI5 702 NGTGIMVS#PMKTNQR -1.57 0.74 2.61	4.4		
YPR095C SYT1 297 AKNKPPLS#PSSFIRT -1.11 0.51 1.45	8.5		
YMR005W TAF4 36 TKPAFNLS#PGKASEL -1.68 0.95 0.43	22.7	22.7	2.4
YMR005W TAF4 49 ELSHSLPS#PSQIKST -1.17 1.35 0.43	0		
YML072C TCB3 1373 YAPVQSAS#PVVKPTD -1.81 0.67 0.43	0		
YML072C TCB3 1350 NLNSTSVT#PRASLDY -1.57 1.04 0.43	158.9		
YPL180W TCO89 546 KNSAAPAS#PLSNEHI -1.86 0.65 0.43	0		
YML064C TEM1 240 SPSSKAPS#PGVNT -1.69 0.65 0.43	16.6		
YKR062W TFA2 97 DDEDFGSS#PSKKVRP -2.23 0.84 0.43	15.4		
YKL140W TGL1 466 RTHSADRS#PLSVQAD -1.88 0.65 0.43	26.5		
YKR089C TGL4 756 SFSFSVAS#PTSRMLR -2.83 0.76 0.43	10.5		
YKR089C TGL4 675 NSTLLTRT#PTKGDNH -1.98 0.65 0.43	73.8		
YGL049C TIF4632 196 TPFEKEAT#PVLPANE -4.68 1.09 1.91	0		
YGL049C TIF4632 301 KSGASVKT#PQHVTGS -1.49 0.51 1.91	19.7		
YNL088W TOP2 1250 TKIKKEKT#PSVSETK -2.52 0.93 0.43	32.4		
YLR183C TOS4 98 KFSSKLSS#PSRHTRV -2.08 0.77 2.85	8	8	4.9
YMR261C TPS3 148 APSARVCS#PSQEASA -1.53 0.61 0.52	748.4		
YER093C TSC11 28 TNTTPLLT#PRHSRDN -2.53 0.63 0.43	22		
YML100W TSL1 77 ISRSATRS#PSAFNRA -2.52 0.60 0.52	20.6		
YML100W TSL1 161 DSGSRIAS#PIQQQQQ -1.28 0.60 0.52	26.9		
YML100W TSL1 147 IPTDRIAS#PIQHEHD -1.26 0.60 0.52	1323.2		
YML100W TSL1 135 GSVERFFS#PSSNIPT -1.07 0.60 0.52	0		
YOR124C UBP2 917 EDTTGLTS#PTRVAKI -1.18 0.63 0.43	3.3	3.3	0.4
YGR184C UBR1 300 PSNSPEAS#PSLAKID -1.13 0.56 0.43	3.4		
YGR184C UBR1 296 AKTSPSNS#PEASPSL -1.13 0.56 0.43	3.4		
YPL020C ULP1 25 NPYSPLFS#PISTYRC -1.62 0.97 1.00	0		
YPL020C ULP1 21 YHKKNPYS#PLFSPIS -1.62 0.88 1.00	0		
YIL031W ULP2 984 IDDVAFSS#PTRGIPR -2.50 0.60 1.67	11.9	16.8	2.2
YIL031W ULP2 795 SPETASVS#PPIRHNI -1.03 0.65 1.67	2.45		
YIL031W ULP2 788 EDPVRAAS#PETASVS -1.03 0.51 1.67	2.45		
YML029W USA1 376 PPDTRSQS#PVSFAPT -1.40 0.77 0.43	10.1		
YIL135C VHS2 301 TGAALSRS#PSNQQYL -1.47 1.04 1.11	24.1		
YOR054C VHS3 225 RSRSNSTS#PRPSVVV -1.48 1.20 1.13	28.3		

(Continued)

Table A2 | Continued

Peptides	Cln	Cln-sum	*P*-score
YLR410W VIP1 1107 FTPVNITS#PNLSFQK -2.33 1.58 0.89	30.4		
YLL040C VPS13 1379 SESERTAT#PQSLQGS -1.32 0.63 0.43	0	0	−10
YLR337C VRP1 703 ISKNPTKS#PPPPPSP -1.24 0.51 0.98	44.9		
YLR337C VRP1 709 KSPPPPPS#PSTMDTG -1.17 0.51 0.98	6.5		
YML076C WAR1 126 KRKPRSRS#PTPFESP -1.03 0.60 0.68	29.5		
YOR083W WHI5 154 RRSEVFLS#PSPRLRS -6.54 1.18 1.11	68.45	256.4	2
YOR083W WHI5 156 SEVFLSPS#PRLRSPP -6.54 1.11 1.11	68.45		
YOR083W WHI5 88 SLQGIFMS#PVNKRRV -2.95 0.99 1.11	11.4		
YOR083W WHI5 161 SPSPRLRS#PPTAARR -2.75 1.18 1.11	102.5		
YOR083W WHI5 62 FGTPSPPS#PPGITKS -1.97 1.12 1.11	2.8		
YOR083W WHI5 57 RLKNGFGT#PSPPSPP -1.97 1.04 1.11	0		
YOR083W WHI5 59 KNGFGTPS#PPSPPGI -1.97 0.65 1.11	2.8		
YHL028W WSC4 541 RTSTFLHS#PIQKQHE -2.25 0.60 1.18	10.6	10.6	−10
YDR369C XRS2 349 RAPEVEAS#PVVSKKR -2.34 0.65 0.43	0	0	−10
YBL005W-AYBL005W-A 409 NVSTFNNS#PGPDNDL -1.03 0.51 0.53	33.1		
YCL019W YCL019W 1014 TVESDTTS#PRHSSTF -1.68 0.51 0.49	31.6	31.6	−10
YDL089W YDL089W 441 NRPSKSLS#PLRKTPL -3.67 1.09 1.07	38.2	145.1	2.7
YDL089W YDL089W 446 SLSPLRKT#PLSARQK -3.67 1.05 1.07	38.2		
YDL089W YDL089W 474 DINSILRS#PKKKKNY -2.40 1.32 1.07	68.7		
YDL156W YDL156W 99 NQLLKMGS#PDGQDKN -1.13 0.64 0.43	5.3		
YDL173W YDL173W 148 SLHATTSS#PNNNAPI -2.33 0.65 0.52	27.1		
YDL173W YDL173W 246 GGAGNIIS#PKSSRNT -1.67 1.05 0.52	65		
YDR089W YDR089W 238 NNSSLPAS#PRSIPLL -1.29 0.95 0.43	11.5		
YDR239C YDR239C 63 APDIPPRS#PNRNAHS -2.10 0.65 0.63	17.5		
YDR348C YDR348C 121 SATDFRRS#PPPVSRN -1.35 0.85 0.64	23.9	23.9	3.5
YEL043W YEL043W 847 RRSFHASS#PPFNSIW -1.12 0.91 0.54	6.1		
YEL043W YEL043W 862 NSNTNQLS#PPLEEQY -1.12 0.51 0.54	6.1		
YER079W YER079W 41 DLDQRSMS#PSNIASG -1.41 0.65 0.43	9.9		
YFL042C YFL042C 149 ATIAEIGS#PLQQVEK -2.44 0.75 0.80	0	151	1.5
YFL042C YFL042C 103 SFKSNVPS#PVSRSTT -1.21 0.65 0.80	31.7		
YFL042C YFL042C 110 SPVSRSTT#PTSPVSQ -1.01 0.65 0.80	119.3		
YGR125W YGR125W 42 RASVSAMS#PPLCRSY -1.11 0.65 0.43	7.2		
YGR237C YGR237C 117 PSKSYLRS#PSVERSR -3.13 0.61 0.47	29		
YHR159W YHR159W 236 HLDPSLNT#PVKNRAF -3.11 0.80 0.81	203.8	259.1	3.4
YHR159W YHR159W 244 PVKNRAFS#PVYQNIP -2.72 0.80 0.81	14.8		
YHR159W YHR159W 29 RNSIISMS#PVRKTGR -2.38 0.77 0.81	28.3		
YHR159W YHR159W 286 TNQSRSVS#PQDIQER -1.02 0.80 0.81	12.2		
YIL024C YIL024C 107 QLMDIPLS#PHTRSNT -1.99 0.65 0.43	13		
YIR007W YIR007W 594 YHDTRAKT#PTPEPSP -1.38 0.97 0.43	10.85		
YIR007W YIR007W 596 DTRAKTPT#PEPSPAS -1.14 0.61 0.43	10.85		
YJL193W YJL193W 247 SGFSRQES#PLPLYEK -3.69 1.01 0.72	19.1		
YKL105C YKL105C 980 SWTFGLPS#PLKRRTS -3.65 0.65 0.62	18.5	18.5	−10
YKR077W YKR077W 147 QPAATAPS#PLVSNII -2.19 0.65 0.58	0	0	−10
YKR077W YKR077W 157 VSNIIKPS#PKKLASP -2.19 0.65 0.58	0		
YLL032C YLL032C 762 NTSQSGAS#PQRHKMP -1.87 0.51 0.58	16.1	16.1	1
YLR049C YLR049C 80 QGSPVAPS#PNHRSTM -1.24 0.59 0.43	0		
YMR086W YMR086W 675 HSAIPLGT#PEKGKPK -3.94 0.77 0.78	364.4	379	−10
YMR086W YMR086W 870 QKENNVVS#PGVSSPN -1.91 0.56 0.78	5.6		
YMR086W YMR086W 658 SIRSNSPS#PPEKINN -1.62 0.79 0.78	9		
YMR124W YMR124W 586 FSSTFSDS#PSKQRII -1.71 0.94 0.83	16.9	16.9	−10
YMR196W YMR196W 1081 IDPMDPMS#PLNKDVS -1.25 0.60 0.43	4.4		
YMR233W YMR233W 113 RKKKKNDS#PDSNSIS -3.86 0.60 0.43	21.4	21.4	−0.2

(Continued)

Table A2 | Continued

Peptides	Cln	Cln-sum	*P*-score
YMR291W YMR291W 538 NEVDLLLT#PRTASMS -1.31 0.65 0.43	0		
YNL058C YNL058C 292 SATSNTSS#PKKAHKR -1.63 0.90 0.62	68.6	68.6	2.3
YNL224C YNL224C 345 NNLLPSPS#PQLTEDI -2.60 0.79 0.43	10		
YNL224C YNL224C 343 ADNNLLPS#PSPQLTE -2.60 0.65 0.43	0		
YNL321W YNL321W 118 VPDLNTAT#PSSPKRM -1.97 0.83 0.43	5.9	11.8	3.7
YNL321W YNL321W 121 LNTATPSS#PKRMHSS -1.97 0.65 0.43	5.9		
YNR047W YNR047W 201 GRRRSPST#PIMPSQN -2.09 1.35 1.32	3.15	48	3.6
YNR047W YNR047W 198 TGTGRRRS#PSTPIMP -2.09 1.09 1.32	3.15		
YNR047W YNR047W 175 REHSNCGS#PIMLSSS -1.56 0.65 1.32	0		
YNR047W YNR047W 339 LKDTLNGS#PSRGSSK -1.48 1.08 1.32	10.2		
YNR047W YNR047W 137 MTSVANAS#PASPPLS -1.38 0.84 1.32	10.5		
YNR047W YNR047W 140 VANASPAS#PPLSPTI -1.00 1.33 1.32	10.5		
YNR047W YNR047W 144 SPASPPLS#PTIPETD -1.00 1.09 1.32	10.5		
YOL070C YOL070C 403 YEDIIEET#PKKTKLK -1.14 0.65 0.61	7.2	7.2	3.1
YOR227W YOR227W 61 VPTKTIAS#PQRPLSG -1.02 0.68 0.72	60.1		
YML027W YOX1 324 NPQKKTLT#PVKTSPN -1.42 1.35 2.07	0	0	2.8
YPL141C YPL141C 441 LSHEQSLS#PVQNIRQ -1.44 0.56 1.55	0	0	−0.9
YPL150W YPL150W 456 YSHSIAGS#PRKSNNF -1.09 0.65 0.71	109.6		
YPR091C YPR091C 676 SQPLNTLS#PKLEGRK -1.13 0.73 1.35	62.8		
YPR115W YPR115W 969 ARRGSDLS#PFEMESP -3.18 0.51 0.80	17.9		
YPR115W YPR115W 975 LSPFEMES#PLFEENR -2.70 0.65 0.80	5.5		
YPR174C YPR174C 170 VNPLVTSS#PIHMSPL -2.85 1.12 0.49	17.6	35.2	2.5
YPR174C YPR174C 175 TSSPIHMS#PLQSRQR -2.85 0.65 0.49	17.6		
YIL063C YRB2 31 PIDKLDGT#PKRPREK -1.24 0.56 0.72	54.4		
YHR016C YSC84 311 EDYDYGRS#PNRNSSR -2.60 0.63 0.43	7.1		
YDR326C YSP2 572 FLNRRSFS#PSNLGNK -1.20 1.08 0.74	52.4		
YNR039C ZRG17 58 QNRTFFAS#PRPSSLF -2.51 1.23 0.76	10.8		
YER033C ZRG8 914 LNRRTLKS#PLRGGSK -4.46 1.20 1.19	32.4	32.4	−10

Column 1: Cdk1-phosphorylated peptides, according to Holt et al. (2009).

Column 2: Average S/N ratios of the phosphopeptides from cells arrested by the overexpression of a stable, mitotic cyclin (Holt et al., 2009). If a phosphopeptide was not detected in this cell population, its ratio is entered as 0 here.

Column 3: Sums of the S/N ratios for every protein. These values are not corrected for Cdk1-dependent phosphorylation (Holt et al., 2009), but such a correction did not alter our conclusion (not shown).

Column 4: P-scores of the proteins determined by Ubersax et al. (2003). If a protein was tested and found not to be phosphorylated, its P-score is entered as −10.